AN ABSTRACT OF THE THESIS OF

Laurance Leroy Oden for the Ph.D. in Physical Chemistry

Date thesis is presented _____*March 1, 1965*_____

Title   INFRARED INVESTIGATION OF SOME FERROELECTRIC
AND RELATED COMPOUNDS: NH_4NCS, $(NH_4)_2SO_4$, $RbHSO_4$, AND
NH_4HSO_4

Abstract approved ████████████████

At liquid nitrogen temperature the spectra of sublimed
films of NH_4NCS, both as phase I (the usual form stable at
room temperature) and phase II (the low temperature form),
exhibit detail usually reserved for gases at low pressures.
In both phases the symmetry of ammonium ion has degenerated
from tetrahedral to a condition of no symmetry.

The observed frequencies of ammonium ion and its
completely deuterated analog were sufficient to calculate
a complete quadratic potential function with which
vibrational frequencies of the partially deuterated species
NH_3D^+, $NH_2D_2^+$, and NHD_3^+ were calculated. The complex
spectrum to which all species contribute was thus assigned.
The number of components observed for some bending
vibrations of the partially deuterated species was
consistent with the hypothesis that species of C_{3v} and C_{2v}
symmetry could occupy their sites on the crystal lattice
in four and six distinguishable orientations, respectively.

The previous observations preclude the possibility that ammonium ion rotates freely in ammonium thiocyanate.

Vibrations of ammonium ion in phase II exhibited 2n components where n was the number of components observed for corresponding vibrations of phase I. From this evidence a likely crystal structure for phase II was deduced.

$(NH_4)_2SO_4$, $RbHSO_4$, NH_4HSO_4, and their deutero-derivatives were studied with respect to their ferro-electric transitions and low temperature spectra. Samples were produced by evaporation of aqueous solutions upon insoluble BaF_2 substrate windows and by mulling with nujol and fluorolube.

The observed multiplicity of the low temperature spectra was assigned on the following bases: (1) equi-point splitting which originates in the exact theory of crystal spectra whenever like ions occupy inequivalent positions on the crystal lattice, (2) site group splitting which may arise for degenerate modes of free ions whenever the site symmetry is less than the point symmetry of the free ion, and (3) factor group splitting which is produced by coupling of like vibrational modes among equivalent ions within a unit cell. Often the number of components and their relative positions were sufficient to differen-tiate among the three sources of multiplicity. It was found that site group splitting was the dominant effect

followed by equipoint and factor group splitting in that order.

First order phase changes in all three compounds were associated with marked and reproducible changes in the spectra which were reversible with temperature inversion. The infrared spectrum was found completely indifferent to second order transitions.

On the bases of spectral changes at their respective Curie points and their low temperature spectra, dielectric polarization in ammonium sulfate, rubidium bisulfate, and ammonium bisulfate was attributed to the existence of oriented systems of hydrogen bonds.

INFRARED INVESTIGATION OF SOME FERROELECTRIC
AND RELATED COMPOUNDS: NH_4NCS, $(NH_4)_2SO_4$,
$RbHSO_4$, AND NH_4HSO_4

by

LAURANCE LEROY ODEN

A THESIS

submitted to

OREGON STATE UNIVERSITY

in partial fulfillment of
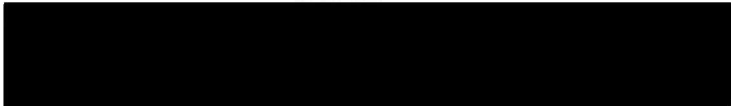the requirements for the
degree of

DOCTOR OF PHILOSOPHY

June 1965

APPROVED:

█████████████████████████
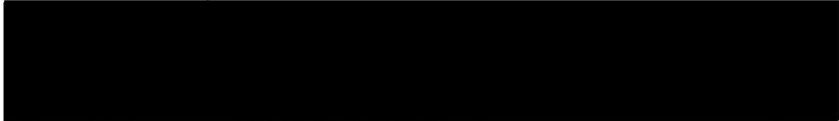
Professor of Chemistry

In Charge of Major

█████████████████████████████

Chairman of Department of Chemistry

█████████████████████████████

Dean of Graduate School

Date of final oral _March 1, 1965_

Typed by Mrs. L. L. Oden

ACKNOWLEDGEMENT

TABLE OF CONTENTS

TABLES

FIGURES

FIGURES continued

INFRARED INVESTIGATION OF SOME FERROELECTRIC
AND RELATED COMPOUNDS: NH_4NCS, $(NH_4)_2SO_4$,
$RbHSO_4$, AND NH_4HSO_4.

I. INTRODUCTION

The discovery of ferroelectricity in compounds
composed of polyatomic species has prompted infrared and
Raman investigations which have sought to learn the
mechanism of the ferroelectric transition. The first
part of the investigations reported here began with
thiourea, a known ferroelectric, and branched off to
ammonium thiocyanate when a previously unreported low
temperature phase was discovered. The spectra of both
the usual and low temperature forms of ammonium thio-
cyanate exhibit remarkable detail at low temperature.
In attempting to understand the detailed spectra,
deuteroammonium thiocyanate was prepared. But, some
samples were only partially deuterated, and their spectra
were exceedingly complex. The spectra were assigned
after the frequencies of the partially deuterated species
had been calculated.

Myasnikova and Yatsenko (21) recorded the infrared
spectra of $(NH_4)_2SO_4$, $RbHSO_4$, and NH_4HSO_4 from mineral
oil mull samples at temperatures to -150° C. They
assigned the spectra and postulated the cause of ferro-
electricity, but some of their assignments and conclus-
ions did not seem justified by their published spectra.

Because of the availability of (1) a higher resolution
infrared instrument, (2) improved sampling technique,
and (3) improved low temperature cell, the above
compounds were reinvestigated with respect to their
ferroelectric transitions and low temperature spectra.
The spectra of the deuterium substituted compounds
were also recorded as an aid in assigning the quite
detailed spectra.

II. EXPERIMENTAL EQUIPMENT

Spectrophotometer

All infrared spectra were obtained with a Beckman IR-7 spectrophotometer which was equipped with NaCl and CsI interchange units. The instrument was self recording and utilized double prism dispersion for preliminary sorting of wave lengths and grating dispersion for fine sorting. In the wave length region 650 to 4000 cm^{-1}, a 60 x 75 mm, 60°, NaCl foreprism was used together with a 64 x 64 mm replica grating ruled 75 lines per mm with 12 micron blaze. The IR-7 was capable of 0.3 cm^{-1} resolution at 1000 cm^{-1} (3, p. 13). In the region 250 to 700 cm^{-1}, a 60 x 75 mm, 48°, CsI foreprism was used in conjunction with a 64 x 64 mm replica grating ruled 30 lines per mm with 30 micron blaze. Resolving power was better than 1.0 cm^{-1} between 290 and 700 cm^{-1} (2, p. 2). Scanning speeds were necessarily slow, 0.8 cm^{-1} per minute, at conditions affording maximum resolving power; therefore, since the sharpest absorption maxima of single crystal spectra seldom have half-band-widths less than two or three cm^{-1}, the IR-7 was usually operated at conditions producing one third to one fourth of maximum performance.

Low Temperature Cells

Pyrex Cold Cell.

For the investigations which involved ammonium thiocyanate, a pyrex low temperature infrared cell was used that was constructed according to the instructions of Wagner and Hornig (36). During the investigations, the cell was improved by adding brass end plates having O-ring grooves for attaching the infrared-transparent windows. Ammonium thiocyanate was observed principally as a polycrystalline film that had been condensed from the vapor onto a rock salt or cesium bromide substrate window. For producing sublimed samples, a double walled pyrex tube was connected to the cell body by standard taper joint in a position perpendicular to the beam path. A nichrome heater was placed between the double walls, and one to two mg of the sample for sublimation was placed within the inner tube. Temperature within the sublimation head was held to the minimum necessary to produce transport of material by carefully controlling the voltage applied to the heater. Samples of ammonium thiocyanate produced in this manner showed no spectro-scopic evidence of pyrolysis. The substrate window, which was secured to the cold finger of the cell in a manner to be described later, could be rotated 90° to receive a film sample and then rotated back into position

within the infrared beam path. Temperature of the
substrate window was measured by a copper-constantan
thermocouple that was embedded within the substrate
window. The pyrex cell, although greatly inferior
to the liquid helium cell to be described later, allowed
us to produce very good ammonium thiocyanate samples
under vacuum conditions, and to record their spectra at
temperatures to about $90^{\circ}K$ without ever exposing the
samples to the atmosphere.

Liquid Helium Cold Cell

A low temperature cell capable of confining liquid
helium was available for investigation of the ferro-
electric sulfates and bisulfates. The cell, which is
illustrated together with its accessories in figure one,
was constructed by Hofman Cryogenics Inc., Hillside, N. J.
according to one of their now standard designs. The
sample holder, heat shield, and sublimation head of the
cell were constructed in our laboratory.

Basically the cell was a double dewar in which
evacuated jackets separated the inner liquid helium
cavity from the surrounding liquid nitrogen reservoir
and the nitrogen reservoir from the cell's exterior.
The helium cavity and nitrogen reservoir terminated in
threaded blocks to which the sample holder and heat
shield, respectively, were attached. Stainless steel

was used in construction of the cell body, and copper
was used for cell accessories which were cooled by
conduction. The lower vacuum jacket, which was secured
by O-ring flange to the main cell body, could be removed
to allow access to sample holder and heat shield. The
lower vacuum jacket was equipped with O-ring seated mounts
in which were placed the infrared-transparent windows.
Windows approximately 1 3/8 inches in diameter were
necessary to cover the O-ring seat through which was
provided a circular beam path 13/16 inch in diameter.

The sample holder accommodated substrate windows or
samples with dimensions 1 inch by 9/16 inch by 1/8 inch
to 1/4 inch. A shoulder prevented the substrate from
passing through the sample holder, and the substrate was
forced firmly against the shoulder by a retaining ring.
The retaining ring was provided with a rectangular opening
13/16 inch by 3/8 inch through which the infrared beam
passed. Indium gaskets were used between shoulder and
substrate and between substrate and retaining ring to
provide good thermal contact.

The heat shield was constructed from thin walled
copper tubing 1 1/8 inches in outside diameter. Thin
copper sheet formed the bottom of the cylinder, and a rec-
tangular hole 7/8 inch x 1/2 inch was milled transversely
through the cylinder in a position to transmit the

infrared beam. The shield was attached by threaded
coupling to the terminal end of the liquid nitrogen
jacket.

The sublimation head consisted of a hollow brass
cylinder 1 1/8 inches long, 7/8 inch in outside diameter,
and 1/2 inch in inside diameter which was fitted with a
pyrex insert for holding the sample to be sublimed. The
brass cylinder was soldered to the lower vacuum jacket
of the cell in a position perpendicular to the infrared
beam path. An O-ring separated the pyrex insert from the
brass cylinder, and atmospheric pressure held the insert
in place when the cell was evacuated. The lower vacuum
jacket of the cell could be rotated at the O-ring
junction with the cell body to position the sublimation
head directly in front of the substrate window. In
subliming position, the lip of the pyrex insert and the
substrate window were separated by approximately 1/2 inch.
The details of construction of the sublimation head are
best illustrated in figure one.

Electrical contacts to a 20 watt heater that was
wrapped onto the helium finger of the cell and to two
thermocouples within the cell were provided by ten
Stupakoff terminals that had been installed by Hofman.
The electrical heater on the helium finger provided
sufficient heat to warm the sample holder from liquid

nitrogen temperature to room temperature in about 15 minutes. The temperature of the helium finger at the position of attachment of the sample holder and the temperature of the heat shield were monitored by copper-constantan thermocouples.
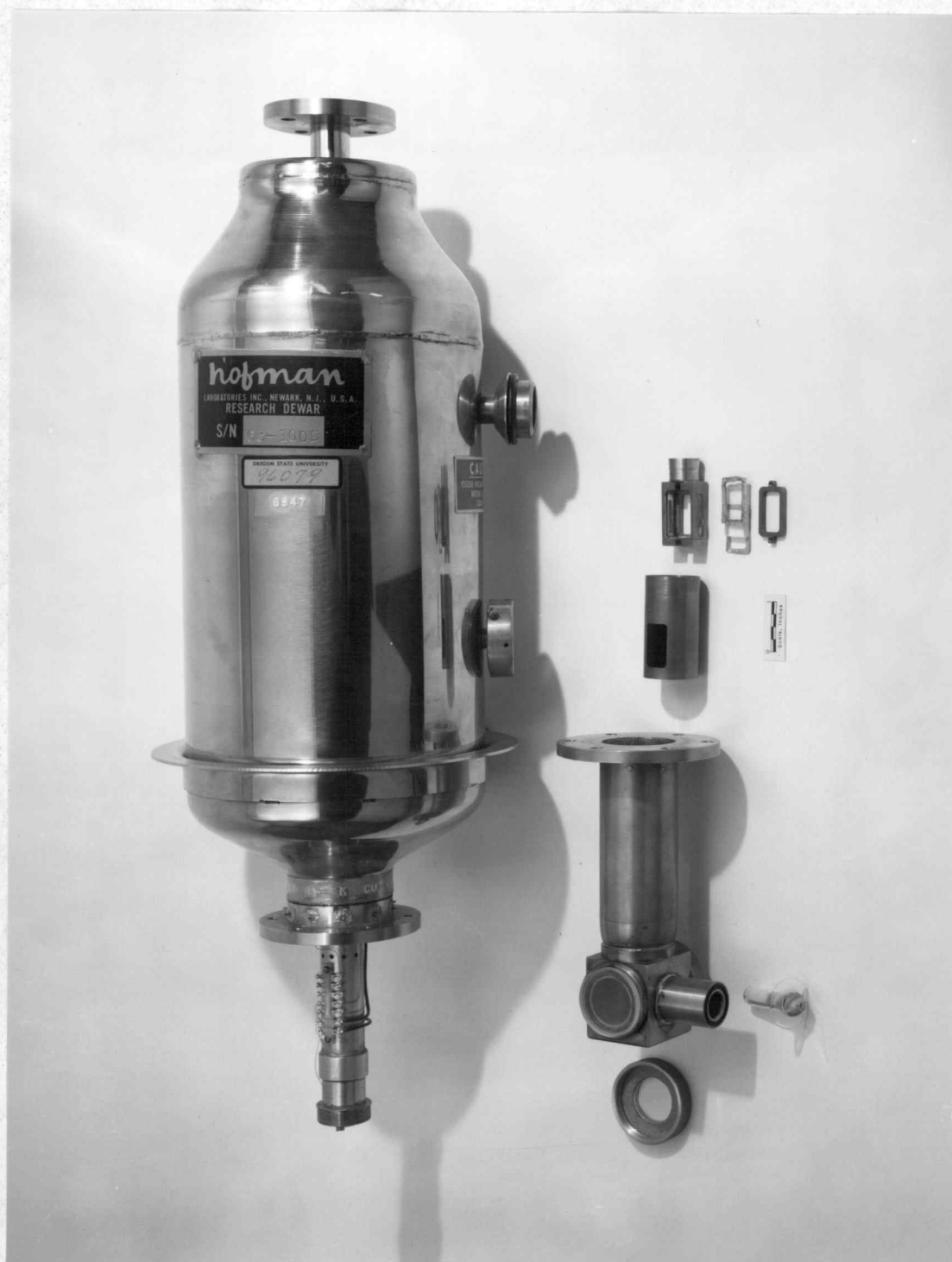
Figure 1. Liquid helium cold cell and accessories

III. EXPERIMENTAL TECHNIQUES

Materials

Reagent grade chemicals were used to produce all samples in this investigation. No spurious absorptions attributable to impurities present in the original reagent grade chemicals were observed.

Deuteration of NH_4NCS, NH_4HSO_4, and $RbHSO_4$ was carried out by multiple recrystallization from 99.6 percent D_2O. Usually three or four crystallizations produced sufficient deuteration for our study.

Sample Preparation

Pressed Alkali Halide Discs

Some preliminary investigations were carried out, in the cases of NH_4NCS, NH_4HSO_4, and $(NH_4)_2SO_4$, using the KBr pelleting technique. Pellet spectra were in general inferior to mull spectra and to the spectra of samples produced by sublimation or solvent evaporation. In the case of NH_4HSO_4, interaction occured between the salt and the pelleting material (KBr, NaCl) to produce spurious absorptions. In general, pellet spectra were of little use.

Mull Technique

Mull spectra were very valuable. Carefully dried salt that had been hand ground in a warm mortar for 10 to 15 minutes and mixed therein with nujol or

fluorolube produced very detailed spectra. Kel-F 10, trademark of the M. W. Kellog Co., Jersey City, N. J. for their low viscosity fluorocarbon oil, is infrared transparent above about 1300 cm^{-1}, and nujol is transparent below about 1350 cm^{-1}; thus, if desired, spectra spanning the infrared region can be recorded from mull samples.

In the case of the ferroelectric materials, the nujol mull spectra are illustrated in the low frequency region. Mull spectra were recorded for comparison purposes in the higher frequency region for the ferroelectric compounds, but they were not selected for illustration because greater detail was observed in the spectra of samples produced by the solvent evaporation technique.

Sublimation Technique

The sublimation technique for sample preparation produced the best samples of NH_4NCS and its deuterated analogs, but the method was not suitable for the ferroelectric compounds because of pyrolysis. Samples were prepared by the following sequence of operations: (1) the sublimation head was charged with from one to two mg of salt, and the cell was assembled and evacuated (either pyrex or liquid helium cell), (2) the substrate window was cooled, and a potential was applied to the

sublimation heater just sufficient to sublime the salt,
(3) after the salt had condensed onto the substrate, the
substrate was rotated into position to transmit the
infrared beam, and the spectrum was recorded. Deuterated
samples were transferred to the sublimation head as the
D_2O solution, and the solvent was evaporated within the
cold cell, of course with the substrate window warm.

Solvent Evaporation Technique

Samples of ferroelectric $(NH_4)_2SO_4$, NH_4HSO_4, ND_4DSO_4,
$RbHSO_4$, and $RbDSO_4$ were prepared by simply painting the
H_2O or D_2O solution onto a BaF_2 substrate window and
allowing the solvent to evaporate. Some experimentation
was necessary to produce samples which had optimum small
crystallite size and which showed a minimum of preferred
orientation. Although BaF_2 is quite insoluble, some
interaction between the substrate and the bisulfates did
occur, as evidenced by the appearance of the 981 cm^{-1} and
the 1104 cm^{-1} modes of the sulfate ion in the bisulfate
spectra. This point will be discussed later.

IV. THE INFRARED SPECTRUM OF AMMONIUM THIOCYANATE

This portion of the thesis has received prior publication in Spectrochimica Acta, volume 20, pages 667 - 674, 1964 (22). The following discussion, although more detailed, closely parallels the journal article.

Ammonium thiocyanate was observed with greatest success as a thin polycrystalline film that had been condensed from the vapor onto a transparent substrate window. Samples were invariably amorphous when condensed at liquid nitrogen temperature, and such samples remained amorphous, as evidenced by the extreme breadth of the absorption bands of their spectra, unless warmed to about 185° K. At that temperature crystallization occured as indicated by marked changes both in position and intensity of the absorption maxima. Recooling produced a sharpening of all absorption bands, and with some samples, a great revelation of fine structure. The form of ammonium thiocyanate produced in this manner was at first thought to be the usual form which is stable at room temperature; however on warming to about 207° K for NH_4NCS and 189° K for ND_4NCS, an irreversible transition occured to produce the usual allotrope of the salt. Recooling of this form produced no further changes, just

the expected sharpening of the infrared spectrum. The form of NH_4NCS which is stable below $207^\circ K$ has been named phase II and the usual form, which is stable to room temperature, phase I. The spectra of phases I and II of NH_4NCS from 300 to 3400 cm^{-1} at $90^\circ K$, are shown in figures two and three. Corresponding spectra for ND_4NCS in the frequency range 700 to 3400 cm^{-1} are shown in figure four. In figure five are shown the spectra in the bending region of a mixture of partially deuterated ammonium ions both as phase I and phase II. The spectra will be discussed in the following order: (1) phase I of ammonium thiocyanate at $90^\circ K$, (2) phase I of partially deuterated ammonium thiocyanate at $90^\circ K$, and (3) phase II of ammonium thiocyanate at $90^\circ K$.

Procedures for the analysis and interpretation of the spectra of crystals were given first by Bhagavantam and Venkatarayudu (4, p. 224 - 258) and then by Halford (10). Later, Winston and Halford (41) showed that the method of Bhagavantam, which considered the motions of the crystallographic unit cell, and the method of Halford, which considered individual molecules within the crystal, could both be derived by considering an arbitrary number of unit cells subject to the Born-Karman boundary conditions. The method used here was suggested by Hornig (13, p. 1063 - 1076) who showed that the active frequencies
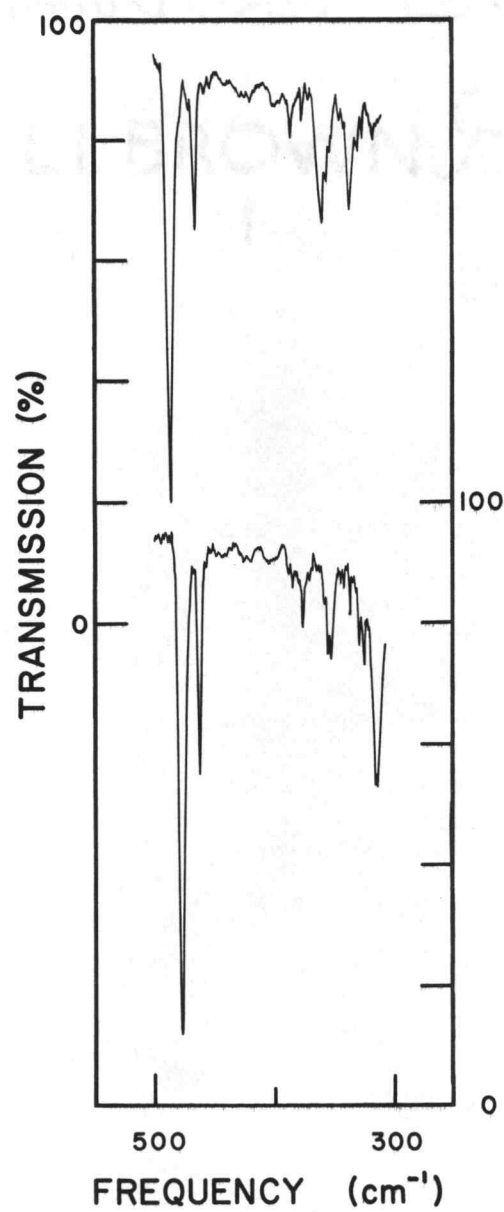
Figure 2. The infrared spectrum of NH_4NCS from 300 to 500 cm^{-1} at 90°K: upper trace phase II; lower trace phase I.
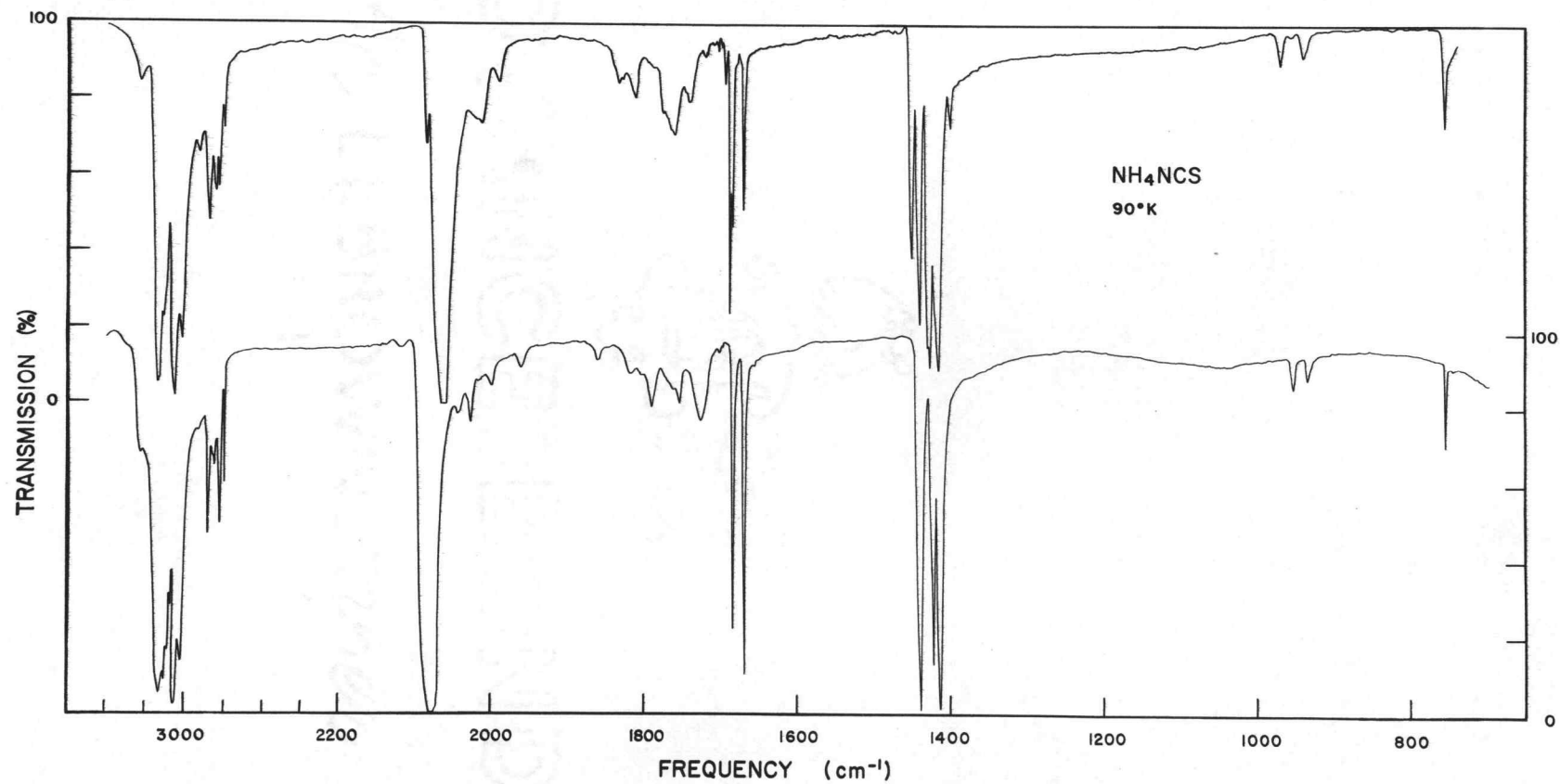
Figure 3. The infrared spectrum of NH4NCS from 700 to 3400 cm^{-1} at 90°K: upper trace phase II; lower trace phase I.
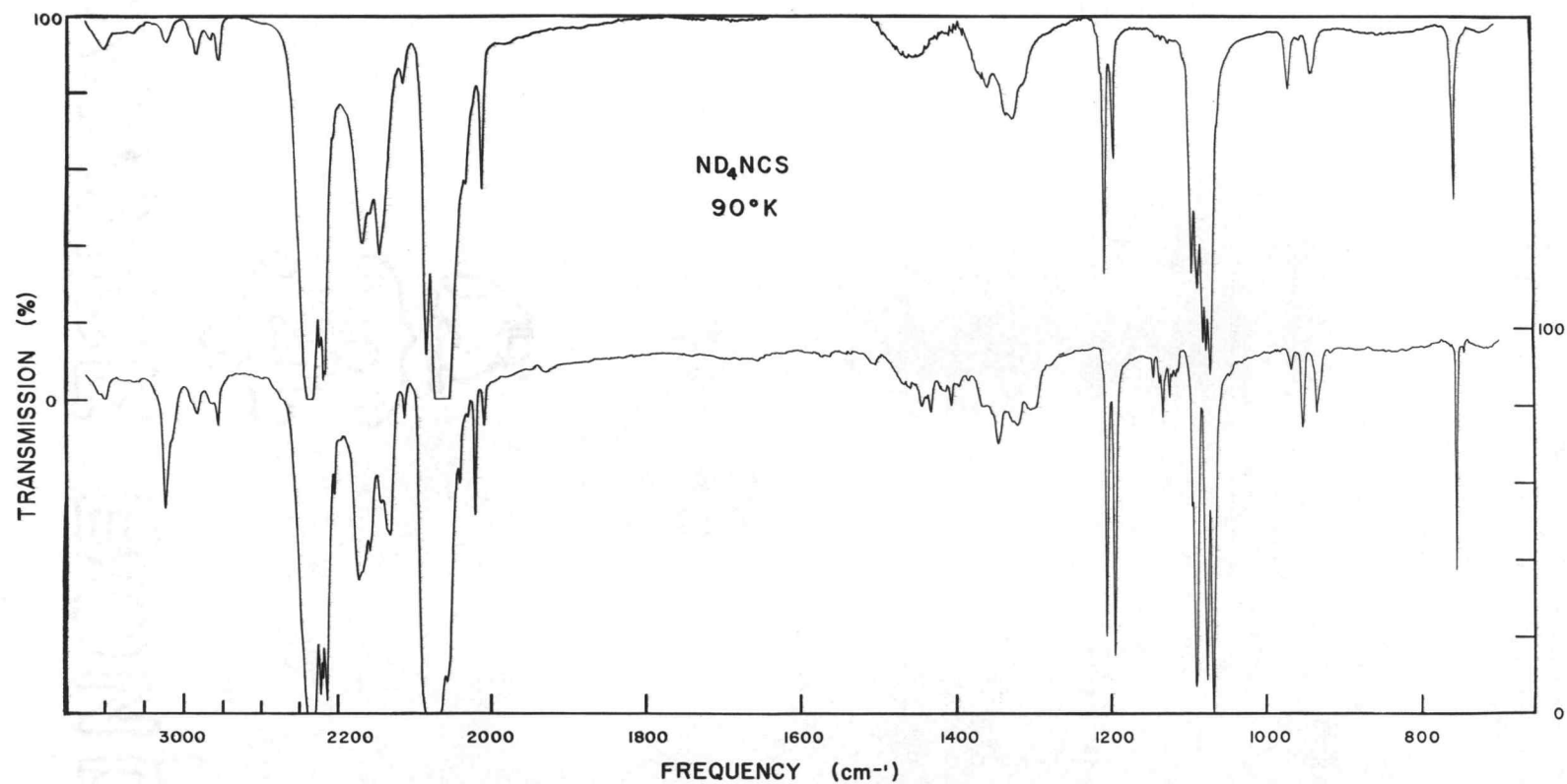
Figure 4.   The infrared spectrum of ND₄NCS from 700 to 3400 cm⁻¹ at 90°K: upper trace phase II;   lower trace phase I.
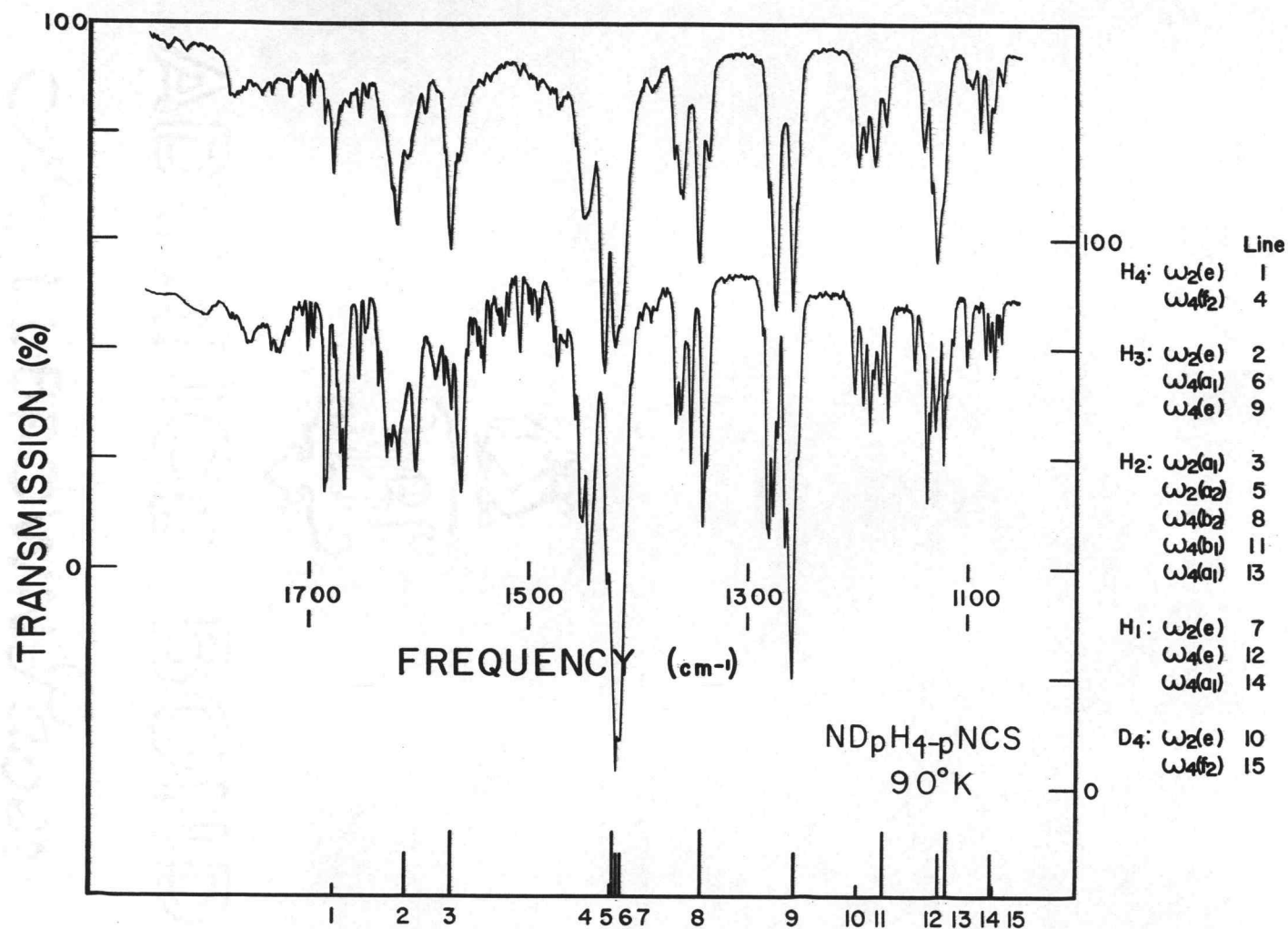
Figure 5. The infrared spectrum of partially deuterated NH_4NCS in the bending region at 90°K: upper trace phase II; lower trace phase I. Calculated spectrum is shown at bottom.

could be calculated from a single unit cell.

To assign the spectrum of crystalline ammonium thiocyanate, it is expedient to follow the sequence of operations: (1) calculate the number of normal vibrations for both ammonium and thiocyanate ions on the basis of their respective free ion symmetries, (2) consider the effects of site symmetry perturbations upon the free ion spectra, and (3) consider the effects of coupling among like vibrational modes of equivalent ions within the unit cell (factor group or unit cell group splitting).

For a free ammonium ion with tetrahedral symmetry, the $3n = 15$ cartesian displacement coordinates form the basis of a reducible representation for the point group of the ion, T_d. The representation so formed contains the irreducible representations, symmetry species, $A_1+E+F_1+3F_2$. On subtracting the contributions to the representation from rotation and translation (F_1 and F_2 species respectively), the remaining symmetry species are pure vibrations, $\Gamma_{vib}= A_1+E+2F_2$. A_1 is a non-degenerate vibration; E is a doubly degenerate vibration, and the F_2 species are triply degenerate. Only those vibrations belonging to F_2 of point group T_d may be active in the infrared.

Thiocyanate ion is linear (16), and as such its

symmetry is described by the elements of point group $C_{\infty v}$. The cartesian displacement coordinates form a basis for the representation $\lceil NCS^- = 3A_1 + 3E$ to which translation and rotation contribute $A_1 + 2E$ species. Thus $2A_1 + E$ are genuine vibrations, and all vibrations are infrared active.

Ammonium thiocyanate (phase I) forms monoclinic crystals, space group $C_{2h}^5 = P\frac{2}{C}1$ (42). The lattice constants of the tetramolecular unit cell are $a_0 = 4.3$, $b_0 = 7.2$, $c_0 = 13.0$, and $\beta = 97^\circ\ 40'$, where all distances are given in angstroms. All ions within a unit cell occupy general positions, and the rank of C_1 equipoints of C_{2h}^5 is four (15, p. 99). Hence all ammonium ions occupy positions within the unit cell which are equivalent by virtue of the symmetry of the unit cell. Similarly all thiocyanate ions are equivalent by virtue of symmetry.

Zvankova (42), using X-ray diffraction, determined the positions of all atoms, excepting protons, within the unit cell. He calculated the distances between the nitrogen atom, designated N, of any given ammonium ion and the sulfur and nitrogen atoms, designated S and N', respectively, of nearest neighbor thiocyanate ions. The dimensions of interest are two equal N – S distances of $3.34\ \overset{\circ}{A}$, one N – N' distance of $3.08\ \overset{\circ}{A}$ and another of $2.99\ \overset{\circ}{A}$. The proton positions are unknown, and hence the

strength of any hydrogen bonds that might exist, between NH and S or NH and N' can only be surmised. However, it can be said with assurance that, due to the small electronegativity of the sulfur atom and the large N - S distance involved, no hydrogen bonding would be expected between NH and S. On the other hand, weak but inequivalent hydrogen bonds may exist between NH and the N' atoms. Hydrogen bonds of this strength would produce no changes in the infrared spectrum that were directly associated with hydrogen bonding (see reference 26, p. 68 for a description of spectral changes associated with the formation of hydrogen bonds). However, the unsymmetrical crystal field in which the ammonium ions reside should distort the free ion tetrahedral symmetry and therefore produce noticeable changes in the infrared spectrum.

A formal treatment which predicts the infrared spectrum of crystalline ammonium thiocyanate from the free ion symmetry, the site symmetry, and the factor group symmetry, respectively, is carried out in figure six.

free ion symmetry	site symmetry	factor group symmetry
T_d	C_1	C_{2h}^5

$A_1 : \omega_1{}^+$

$E : \omega_2{}^+$

$F_1 : \text{Rot.}$

$F_2 : \omega_3{}^+, \omega_4{}^+, \text{Trans}$ — A

$C_{\infty v}$

$A_1 : \omega_1{}^-, \omega_3{}^-$

$E : \omega_2{}^-$

Ag (R)

Bg (R)

Au (IR)

Bu (IR)
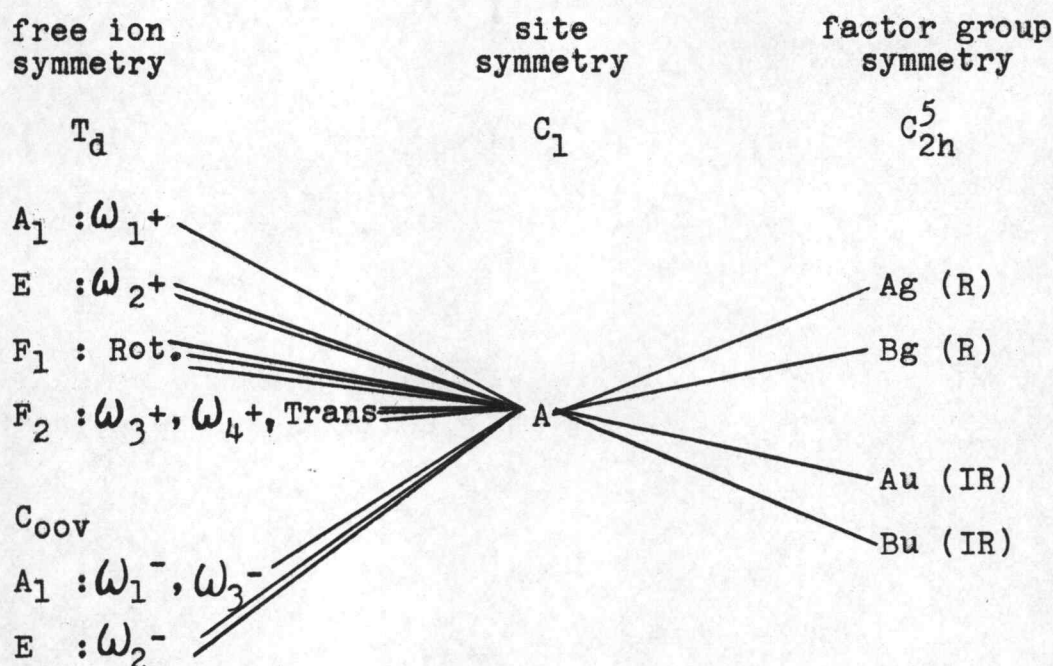
Figure 6. Correlation of symmetry species for crystalline ammonium thiocyanate (Phase I)

The correlation of free ion symmetry with site symmetry reveals that the perturbation of C_1 site symmetry may activate all free ion modes as well as remove all degeneracies for both ammonium and thiocyanate ion vibrations. Further correlation with factor group symmetry results in a quadruplet splitting of all modes. This splitting results from coupling of like vibrational modes among equivalent ions within a unit cell. Since only Au and Bu species of C_{2h}^5 may be active in the infrared and only Ag and Bg active in the Raman, the factor group effect observable using any one technique

is reduced to a doublet splitting.

When an ion becomes part of a crystal and takes a fixed position in the lattice, it forfeits three translational and three rotational degrees of freedom which become the crystal lattice modes of translatory and rotary origin respectively. For the ammonium ion, translation and rotation are both triply degenerate species, F_2 and F_1 respectively. For the thiocyanate ion, translation and rotation each contribute A_1+E species. Translation and rotation have been included in the correlation diagram to show the effects of site symmetry perturbations and factor group splitting. It is known that the lattice modes have frequencies quite low in comparison with the intrinsic vibrations of ions, and as such only a limited number of the lattice modes were observable with the equipment used in this investigation.

Hornig (13) has shown that, in the harmonic oscillator approximation, the number of frequencies active in the infrared or Raman spectrum is just that number calculated on the basis of a single unit cell. Therefore, to the extent that the approximations are valid for the ammonium thiocyanate crystal, all possible fundamental frequencies have been discovered. Of course, numerous combinations and overtones are expected in the actual

spectrum even though these are forbidden in the harmonic oscillator approximation.

There is well-documented proof in the literature (8, 36, 37), to support the existence of site group splitting of the degenerate modes of the ammonium ion; however such proof is lacking in the case of factor group splitting. The relative magnitude of the two effects has been the subject of much discussion (7, 12, 19, 33, 43), and it is generally agreed that the perturbation of site symmetry has larger effect than does coupling of vibrational modes. Thus, assignments will be made first on the basis of site group splitting, and second on the basis of factor group splitting. In table I, components due to the former splitting are designated by small case letters. No splitting due to factor group effects was observed; hence no system of designation was necessary.

TABLE I

OBSERVED FREQUENCIES OF AMMONIUM THIOCYANATE IN PHASES I AND II AT APPROXIMATELY 90°K

Assignment	NH_4NCS Phase I	A.Tramer (35) IR	A.Tramer (35) R	Phase II	ND_4NCS Phase I	Phase II
ω_{Ra}^{+}	315		300	335		
b	354			357		
c	375					
ω_{2a}^{-}	464		465	466		
b	478		479	487		
ω_{1}^{-}	757	752,755	753	756	756(746^{34}S?)	755
$2\omega_{2}^{-}$	936	937	945	940	936	938
	955	951		970	954	968
ω_{4a}^{+}	1414		1405	1400	1069	1060
				1415		1071
b	1423	1420	1409	1425	1078	1077
				1429		1080
c	1439		1445	1439	1091	1088
				1451		1095
ω_{2a}^{+}	1670	1670	1668	1669	1196	1195
				1683		1205
b	1685		1686	1686	1206	1207
				1693		1211
	1727	1750		1720	1302	1311
	1753			1740	1321	1324
	1762			1759	1346	1333
$\omega_{4}^{+}+\omega_{R}$	1770			1774	1365	1356
	1791			1788		
	1805			1810	1400(NHD_3^{+})	1450
	1817			1832	1450	
	1961	1965		1988		
	1998	2010				
$\omega_{3}^{-}(^{13}c)$	2025	2020		2010	2020	2010
	2044					
ω_{3}^{-}	2079	2072	2062	2060	2075	2060
		2083	2073	2085		2083
	2800	2815		2800	2113	2113
	2825*				2131	
$2\omega_{4}^{+}$	2850	2860			2142	2143
	2858*				2152	2156
	2885			2875	2172	2165
ω_{1}^{+} and	2931			2920		
	3023			3011	2212	2215
$\omega_{2}^{+}+\omega_{4}^{+}$	3056	3047	3050	3054	2252	2253
	3078					2264
ω_{3}^{+}	3091			3096	2275	2270
	3107			3106	2288	2275
	3131	3120	3140	3134	2336	2334
	3228	3215	3220	3222		
NHD_3^{+}					3090	3086

*vacuum grease

Phase I at 90°K

Tramer (35) has studied various thiocyanates, including ammonium thiocyanate, both by infrared absorption and using the Raman effect. The frequencies and assignments for phase I of ammonium thiocyanate listed in table one, are in general agreement with Tramer's work which is also listed for comparison.

The Ammonium Ion

Wagner and Hornig (36), on investigating the ammonium halides, postulated the existence of a torsional mode of the ammonium ion, ω_R, which can be described as libration around the three orthogonal two fold axes of the tetrahedral model. They never observed the fundamental mode, but they did record two combination modes involving it, $\omega_2^+ + \omega_R$ and $\omega_4^+ + \omega_R$, on the basis of which they calculated the frequency to be 390 cm^{-1} for NH$_4$Cl and 280 cm^{-1} for ND$_4$Cl. Because of lower site symmetry in the case of ammonium thiocyanate (C$_1$ vs. T$_d$ for NH$_4$Cl), the fundamental librational mode is activated, and its three components are actually observed at 315, 354, and 375 cm^{-1} in figure two. The mode is also observed in combination with ω_4^+ as a series of lines extending from 1727 to 1817 cm^{-1} and from 1302 to 1365 cm^{-1} for NH$_4^+$ and ND$_4^+$ respectively. The combination $\omega_2^+ + \omega_R$ may also occur and explain the frequencies observed in the region

of 2000 cm^{-1} for NH_4^+ and 1425 cm^{-1} for ND_4^+.

The triply degenerate bending mode of NH_4^+, an F_2 species, appears as a strong trio of lines at 1414, 1423, and 1439 cm^{-1}; while the corresponding series for ND_4^+ appears at 1069, 1078, and 1091 cm^{-1}. ω_4^+ is one of the infrared active modes of the free ion, and as such it could be expected to be very strong in the crystal spectrum; this is indeed seen to be the case. On the other hand, the doubly degenerate bending mode ω_2^+, which is an E species, is inactive for the free ion and is only activated by the perturbation of the asymmetric crystal field in which the ammonium ion resides. Both components of ω_2^+, as predicted by site splitting, are observed at 1670 and 1685 cm^{-1} for NH_4^+ and at 1196 and 1206 cm^{-1} for ND_4^+. Since there is but one E mode in the ammonium ion spectrum, the product rule can be applied to ω_2^+ :

$\dfrac{\omega_2^+(D)}{\omega_2^+(H)}$ = 0.716, which is in good agreement with the

theoretical value, 0.707.

The combination mode $2\omega_4^+$ appears strongly in the region of 2850 cm^{-1} for NH_4^+ and 2140 cm^{-1} for ND_4^+. The pair of lines at 2825 and 2858 cm^{-1} appear in many spectra. Their intensities and frequencies are temperature independent; hence they are thought due to hydrocarbon vacuum grease on the observation windows of the cold

cell. A combination mode of the thiocyanate ion, to add a further complication, also occurs in this frequency region.

The value for the frequency of the band center of the combination mode $\omega_2^+ + \omega_4^+$, obtained by merely summing the observed fundamental frequencies, is 3118 cm^{-1} for NH_4^+ and 2280 cm^{-1} for ND_4^+ which places it in the respective N - H or N - D stretching region. The combination mode would be expected to be rather weak in comparison with ω_3^+, which is the triply degenerate stretching vibration, the strongest of the ammonium ion vibrations. But, the stretching region is the most complex of the spectrum and consists of two main branches of nearly equal intensity. Wagner and Hornig (36), in the case of ammonium chloride, also observed two main equi-intensity components in the stretching region which they attributed to Fermi resonance between $\omega_2^+ + \omega_4^+$ and ω_3^+ with the combination mode borrowing intensity from the strong fundamental. ω_3^+ for ammonium thiocyanate should be a strong triplet, evoking only site group splitting, and $\omega_2^+ + \omega_4^+$ may have six components. Thus there may be a maximum of nine components if Fermi resonance prohibits accidently degenerate energy levels from being coincident. Also contributing to the complexity of the region is ω_1^+, an A_1 species, which is

inactive for the free ion but may well be activated here. This mode is observed at 3050 cm^{-1} in the room temperature Raman spectrum of NH_4NCS (35). The possibility of ten components accounted for above is sufficient to explain the seven components actually observed for NH_4^+ and the five observed for ND_4^+. Furthermore, since anharmonicity invariably results in a decrease of frequency from that predicted by the harmonic oscillator approximation, it is reasonable to assign the lower frequency branch to the combination mode $\omega_2^+ + \omega_4^+$. The higher frequency branch is then logically assigned to the fundamental, ω_3^+. In view of the evidence from the Raman spectrum, the mode of 3056 cm^{-1} is probably ω_1^+ of NH_4^+.

Assuming that the strong fundamental ω_3^+ is only slightly shifted by the resonance interaction, its band center may be used to apply a product rule check to the two F_2 species.

$$\frac{\omega_3^+ (D) \quad \omega_4^+ (D)}{\omega_3^+ (H) \quad \omega_4^+ (H)} = 0.564$$

The theoretical value is 0.5528. In view of the good agreement of the product rule, there can be no doubt in the assignment of ω_4^+ or in the general assignment of ω_3^+.

The observed vibrational frequencies of NH_4^+ and ND_4^+ are sufficient to calculate a complete quadratic potential function for the ammonium ion. The calculations

were carried out in appendix I using a modification of Wilson's FG matrix method (39) that was suggested by Decius (6). Wilson's method involved definition of the potential and kinetic energy as quadratic forms which lead to solution of a secular equation $|FG - \lambda E| = 0$. But Decius has shown that the form $|KC - \Phi E| = 0$ often has advantages, and it is this form that was used in the calculation. K is the matrix inverse of G; and C, the compliance matrix, is the inverse of F, the force constant matrix. F of course completely characterizes the potential energy of a molecule in the harmonic oscillator approximation. The eigenvalues of KC are related to the frequencies of vibration in wave numbers, ω, by the relation $\phi_i = 1/4\pi^2 c^2 \omega_i{}^2$, where C is the speed of light.

For the tetrahedral, XY_4, model the compliance matrix contains seven different elements. In terms of internal coordinates comprised of four Δr's and six ΔR's, where Δr and ΔR designate small changes in XY and YY distances respectively, the elements of the compliance matrix are defined as follows: C_r and C_R are the diagonal elements associated with XY and YY stretches respectively; C_R' and C_R'' are coupling constants connecting two different YY stretches which have or do not have an atom in common; C_r' is a coupling constant for two different XY stretches; C_{rR} and C_{rR}'

refer respectively to coupling of XY with YY stretches which do and do not possess a common atom. The frequencies and compliance constants, as calculated in appendix I, are tabulated in table II. Actually, instead of using the value of ω_1^+ available from the Raman spectrum, ω_1^+ was calculated from the 3090 cm^{-1} mode of NHD$_3^+$ and ω_3^+ of NH$_4^+$. The calculated value, 3138 cm^{-1}, appears to be too high, an error, if it is an error, for which no immediate explanation is available. Even if the frequency is in error, the calculated low frequency modes in the bending region will not be appreciably affected, and since this is the region of interest, the compliance constants were not refined using the Raman frequency.

TABLE II

AVERAGE OBSERVED FREQUENCIES AND COMPLIANCE CONSTANTS FOR AMMONIUM ION IN CRYSTALLINE AMMONIUM THIOCYANATE (PHASE I)

Frequency	NH$_4^+$	ND$_4^+$	Compliance Constant Å/millidyne	NH$_4^+$	ND$_4^+$
ω_1^+	3138*	2219*	C_r	0.2080	0.1987
ω_2^+	1677.1	1201.0	C_r'	-0.0118	-0.0088
ω_3^+	3070	2292	C_R	0.6464	0.6414
ω_4^+	1425.2	1078.6	C_R'	0.0143	0.0168
			C_R''	-0.0141	-0.0191
			C_{rR}	0.1150	0.1113
			C_{rR}'	0.0258	0.0295

*calculated value

Either due to a leak in the cold cell or the presence of adsorbed water within the cell, the proportion of residual hydrogen in the deuterated samples always increased when the cell was allowed to warm from liquid nitrogen temperature. The species most probably formed by the introduction of very small amounts of hydrogen is NHD_3^+. Thus the NH stretching region of the phase I spectrum of ND_4NCS shows a single component at 3090 cm^{-1}, and the bending region of the same spectrum shows lines near 1150 cm^{-1} which are probably due to NHD_3^+ as a relatively dilute solution in ND_4^+. To substantiate this hypothesis and investigate the spectrum of all the partially deuterated species, the theoretical spectra were calculated and compared with the observed spectrum of a sample containing approximately one-half deuterium. These results will be discussed in the next section.

Partially Deuterated Ammonium Ion

Partial deuteration destroys the tetrahedral symmetry of the ammonium ion, and the spectra of species so produced are considerably more complex than the spectrum of the tetrahedral ion. Further complexity in the spectrum arises because no one partially deuterated species can be observed alone. Figure five shows the spectrum, in the bending region, of a sample that

contained approximately half deuterium. Assuming a 50 percent concentration, then the relative abundance of species NH_4^+, NH_3D^+, $NH_2D_2^+$, NHD_3^+, and ND_4^+ is 1:4:6:4:1. Due to the complexity of the spectrum of the mixture of ions, any plausible assignment must surely be based on calculations.

Replacement of either one or three hydrogen atoms by deuterium reduces the tetrahedral symmetry of the ammonium ion to C_{3v}, and replacement of two hydrogens results in a C_{2v} structure. Since C_{3v} and C_{2v} are subgroups of T_d, the symmetry species of C_{3v} and C_{2v} can be obtained from the representation for T_d by application of the correlation theorem (40, p. 121-125).
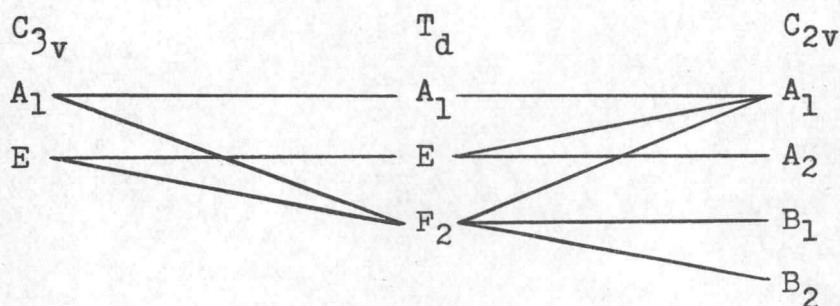
Figure 7. Correlation table between T_d and its subgroups C_{3v} and C_{2v}

Thus $\Gamma C_{2v} = 4A_1 + A_2 + 2B_1 + 2B_2$ and $\Gamma C_{3v} = 3A_1 + 3E$. In the crystal, the perturbing influence of site symmetry and factor group splitting remain to be considered. Quite analogously to the ammonium ion

spectrum, site group splitting will undoubtedly break the degeneracy of E modes of C_{3v}, and also, since no factor group splitting was observed for the ammonium ion, none is expected here.

The vibrational frequencies of the partially deuterated species, as listed in table III, were calculated in appendix II using Decius' (6) compliance scheme and compliance constants adjusted by equation one.

$$(1) \quad C_{H_pD_{4-p}} = (PC_{H_4} + (4-P)C_{D_4})/4$$

TABLE III

CALCULATED UNPERTURBED FREQUENCIES OF AMMONIUM ION
FOR VARYING DEGREES OF D-H ISOTOPIC SUBSTITUTION

	NH_4^+	NH_3D^+	$NH_2D_2^+$	NHD_3^+	ND_4^+
ω_1^+	a_1 3138	a_1 3126	a_1 3120	a_1 3138	a_1 2219
ω_2^+	e 1677	e 1613	a_1 1572	e 1417	e 1201
			a_2 1425		
ω_3^+	f_2 3070	a_1 2257	a_1 2247	a_1 2237	f_2 2292
		e 3083	b_1 3098	e 2284	
			b_2 2276		
ω_4^+	f_2 1425	a_1 1421	a_1 1120	a_1 1079	f_2 1079
		e 1258	b_1 1177	e 1126	
			b_2 1344		

The frequencies falling within the range 1100 cm^{-1} to 1900 cm^{-1}, the bending region, are entered at the bottom of figure five. Line heights, as indications of intensities, depict only the relative abundance of the isotopic species, and it is realized, of course, that the true intensities may differ considerably from the simple 1:4:6:4:1 relationship.

Satisfying agreement is noted between the calculated band centers and the observed groups of lines especially in the case of isolated lines such as numbers eight and nine. Unfortunately, atmospheric absorption has complexed the spectrum in the vicinity of lines one, two and three; and additional hydrogen has entered the phase I sample beyond the 50:50 proportion.

An explanation for the number of components of each vibration follows by considering the possible distinguishable orientations that a given ion may assume when confined to a site on the crystal lattice. For example, NH_3D^+ may occupy its site in four distinguishable orientations, and $NH_2D_2^+$ may take any of six different orientations. Thus, nondegenerate modes of the C_{3v} model, A_1 species, may have four components, and E modes may have eight components. Nondegenerate modes of C_{2v} may have six possible components. Reference again to the

crystal structure data of Zvankova (42) reveals that for the NH_3D^+ ion, two orientations may be nearly the same (degenerate) because of the two equal N - S distances. The N - N' distances produce stronger interactions and result in two definitely nonequivalent orientations. Thus, the number of components for nondegenerate modes of C_{3v} and C_{2v} may be reduced to three and four respectively, and E modes of C_{3v} may have six components. Furthermore, an estimate of relative intensities can be made based solely on the relative population of orientations, ie., the component corresponding to the degenerate orientation should be roughly twice as intense as the other components. Also, since additional constraints tend to increase bending frequencies, the most intense component should occur on the low frequency side of the band. Lines eight and nine offer real tests to the hypothesis; line eight, $\omega_4(b_2)$ of $NH_2D_2^+$, shows five clearly resolved components two of which are on the low frequency side and have very nearly the same frequency. Line nine, $\omega_4(e)$ of NH_3D^+, has six components the strongest of which are on the low frequency side, exactly as predicted above. The remaining bending frequencies are quite badly overlapped, but, even so, no exceptions to the hypothesis above are apparent in the spectrum.

Another point of interest that can be proven from the spectrum of figure five is that the ammonium ion does

not undergo free rotation in the crystal. Free rotation
would render all orientations equivalent and collapse
the fine structure to a single line.

The Thiocyanate Ion

The spectrum of the thiocyanate ion has been
investigated in detail by Jones (16, 17), and hence it
deserves only a very brief discussion here. The two A_1
fundamentals, ω_1^-, and ω_3^-, are seen in figure three at
757 cm^{-1} and 2079 cm^{-1}, respectively. ω_1^- is predominantly
S -C stretching; while ω_3^- is C - N stretching. The weak
line observed at 2025 cm^{-1} is ω_3^- for thiocyanate ions in
which the naturally occuring ^{13}C isotope has replaced ^{12}C.
The bending mode, ω_2^-, is a doubly degenerate (E species)
vibration of the free ion, but in the crystal the degeneracy
is broken. Both components, ω_{2a}^- and ω_{2b}^-, are observed at
464 and 478 cm^{-1}, respectively, in figure two.

The combination $\omega_1^- + \omega_3^-$, whose frequency would be
2836 cm^{-1} by simply summing the fundamental frequencies,
falls within a region complicated by $2\omega_4^+$ of the ammonium
ion, and hence it is not discernable in the spectrum. The
overtone modes $2\omega_{2a}^-$ and $2\omega_{2b}^-$, as well as the combination
$\omega_{2a}^- + \omega_{2b}^-$, should also occur in the spectrum. In the
order mentioned, the frequencies obtained from the
fundamentals are 928, 956, and 942 cm^{-1}. But only two
components, 936 and 955 cm^{-1} are actually observed which
are then logically assigned to $\omega_{2a}^- + \omega_{2b}^-$ and $2\omega_{2b}^-$,

respectively. However, Jones (17) has shown unequivocally
for KNCS, in which thiocyanate ions lie in planes of
symmetry, that the two components are $2\omega_{2a}^-$ and $2\omega_{2b}^-$.
He used single crystal samples and polarized infrared
radiation, and as such his conclusions seem irrefutable.
We subscribe to the same assignment; although it
indicates a divergence of the ω_{2a}^- progression instead
of the usual convergence.

Phase II at 90°K

Ammonium thiocyanate, when condensed as an amorphous film from the vapor state at low temperature, forms phase II when allowed to warm to about 185°K. This phase has not been reported in the literature. It is known from experiments with films condensed on substrate windows having various faces exposed, ie., NaCl 100, NaCl 111, CaF_2 100, KB_r 100, and CsB_r 100, and from experiments in which the substrate was rotated with respect to the infrared beam that the spectrum of phase II does not result from an orientation effect. Phase II then must be a crystalline modification of ammonium thiocyanate, and as such it provides an opportunity to suggest a crystal structure based solely on the infrared spectrum.

First of all, the differences in the spectra of phases I and II consist of (1) greater splitting or multiplicity of lines in phase II and (2) small shifts in line positions. The two bending modes of the ammonium ion, ω_2^+ and ω_4^+, show two and three components in phase I and exactly twice as many components in phase II. Since the spectra of phases I and II are very similar, the two crystal structures must be closely related, and no new assignment beyond accounting for

increased multiplicity and shifts in position is called for.

In phase I there are four molecules per C_{2h}^5 unit cell, and all ions occupy general positions (42). Because the rank of C_1 equipoints of C_{2h}^5 is four (15, p. 99), all like ions are equivalent by virtue of the symmetry of the unit cell. If, to form phase II, the symmetry of the unit cell of phase I was partially destroyed so that C_1 equipoints had rank two, then, still maintaining four molecules per unit cell, there would be two pairs of like ions per unit cell. Since the vibrational frequencies of ions in a crystal lattice are perturbed by the crystal field, ions in equipoints unrelated by unit cell symmetry should have slightly different vibrational frequencies. Thus every frequency of the free ion should appear as a doublet in the crystal spectrum even before considering site group splitting. With the latter effect included, A_1, E, and F_2 modes could exhibit a maximum of two, four, and six components respectively, and this is in quantitative agreement with the observed spectrum of the bending modes of the ammonium ion in phase II at $90^{\circ}K$.

A natural relation between the structures of phases I and II, since spectral evidence indicates that the structures are similar, is for the space group of

phase II to be a subgroup of phase I. Three possibilities exist for the space group of phase II if it is to be a subgroup of the space group of phase I, and these relationships are best illustrated by the use of Herman-Mauguin symbolism. Phase I is $C_{2h}^5 = P_c^2 1$ for which P1, P$\bar{1}$, P2$_1$, and Pc are subgroups. The first subgroup deserves little consideration because the rank of its C_1 equipoints is one. But the latter three subgroups are possibilities since the rank of their C_1 equipoints is two. Thus either of the spacegroups P$\bar{1}$, Pc, or P2$_1$, results in a structure that is consistent with the infrared spectrum. Unfortunately, the spectra can not be used to distinguish among the three possibilities.

To summarize the section, the spectrum of phase II of ammonium thiocyanate is consistent with the crystal structures P$\bar{1}$, Pc, or P2$_1$ with four molecules per unit cell. In these structures like ions are equivalent in pairs if ions occupy only general positions. The ammonium ion bending modes are most sensitive to the low symmetry of the unit cell and exhibit the predicted splitting into four and six components for ω_2^+ and ω_4^+, respectively. The thiocyanate frequencies show fewer changes, but do exhibit a marked shift of position in phase II.

Summary

At liquid nitrogen temperature the spectra of sublimed films of NH_4NCS, both as phase I (the usual form stable at room temperature) and phase II (the low temperature form), exhibit detail usually reserved for gases at low pressures. In both phases, the tetrahedral symmetry of ammonium ion has degenerated from tetrahedral to a condition of no symmetry.

The observed frequencies of ammonium ion and its completed deuterated analog were sufficient to calculate a complete quadratic potential function with which vibrational frequencies of the partially deuterated species NH_3D^+, $NH_2D_2^+$, and NHD_3^+ were calculated. The complex spectrum to which all species contribute was thus assigned. The number of components observed for some bending vibrations of the partially deuterated species was consistent with the hypothesis that species of C_{3v} symmetry, NH_3D^+ and NHD_3^+, could occupy their sites on the crystal lattice in four distinguishable orientations, and that the C_{2v} specie, $NH_2D_2^+$, could take any of six distinguishable orientations. The previous observations preclude the possibility that ammonium ion rotates freely in crystalline ammonium thiocyanate. However, three components of a low frequency mode were observed which were attributed to

libration around the three, orthogonal, two fold axes
of free ammonium ion.

Vibrations of ammonium ion in phase II of NH_4NCS
exhibited 2n components where n was the number of
components observed for corresponding vibrations of
phase I. From this evidence, a likely crystal structure
for phase II was deduced.

V. THE INFRARED SPECTRA OF SOME FERROELECTRIC SULFATES AND BISULFATES

Ammonium Sulfate

Because of its specific heat anomaly at -49.5°C, ammonium sulfate was the subject of many investigations long before Matthias (20) discovered its ferroelectric properties in 1956. Pohlman (27) in 1932 and Guillien (9) in 1939 studied the infrared spectrum and dielectric properties, respectively, in relation to the specific heat anomaly. More recent dielectric and thermal studies have been conducted by Couture (5) and by Pepinsky's group at the Pennsylvania State University (14). In the latter study they suggested, on the basis of the following observations, that the ferroelectric transition was first order: (1) the plot of P_S (spontaneous polarization) versus temperature had an abrupt discontinuity at the transition temperature (often called the Curie point and designated Tc); (2) the appearance of a latent heat of transformation, $\Delta H = 0.93$ Kcal / mole; (3) crystals often shattered when cooled through the transition temperature which indicated a large and abrupt variation of the lattice constants at Tc.

Our very disappointing investigations with single crystal infrared samples are in agreement with the last

of their observations. We prepared three or four single crystals which gave acceptable spectra at room temperature but which shattered and were lost completely when cooled through the ferroelectric Curie point. Thus, we were forced to the methods of solvent evaporation and mulling with nujol or fluorolube for sample preparation. Of course, samples so produced were polycrystalline which severely limited the evidence that could be obtained from them.

At least three separate Raman investigations of single crystal ammonium sulfate have been undertaken (1, 32, 34,). Stekhanov and Gabrichidze (32) observed anomalous shifts in some of the Raman frequencies at the Curie point. They attributed the shifts to shortening of hydrogen bonds, N-H ---O with decreasing temperature. They concluded that the hydrogen bond played an important role in the appearance of ferroelectricity in ammonium sulfate. The Raman frequencies reported by Ananthanarayanan (1), are listed in table IV.

In addition to Pohlman (27), Myasnikova and Yatsenko (21) carried out an infrared investigation to determine the mechanism of the ferroelectric transition. They prepared mull samples and observed the spectrum to -130°C. Their conclusion was that ferroelectricity

in ammonium sulfate may not result from hydrogen bonding.

Okaya (23), in an X-ray investigation, found both room temperature and ferroelectric phases to be orthorhombic and that no changes in lattice constants occured at the Curie point. He found the structure at room temperature to be Pnam with cell constants $a_0 = 7.729$, $b_0 = 10.560$, and $c_0 = 5.951$. Below the Curie point the mirror plane was lost, and the space group became Pna2$_1$. All distances were given in angstrom units and the modern convention for designating crystallographic axes was used, ie., c<a<b. The polar axis was found to be the crystallographic c axis.

The most recent and authorative investigation has been an X-ray and neutron diffraction study by Singh (31) who was primarily interested in determining the relationship between the crystal structure and the mechanism of the ferroelectric transition. He determined the positions of all atoms within the unit cell using neutron diffraction for the x and y coordinates and estimating the z coordinates from X-ray data. He found the room temperature structure to be a statistical mixture of two enantiomorphous states which produced a pseudomirror at $z = \frac{1}{4}$. Thus, he concluded that the true symmetry of the room temperature phase was Pna2$_1$ and not Pnam as reported previously. Below Tc, the space group remained

unchanged.

According to Singh the two ammonium ions, which
are crystallographically unrelated, also have different
surroundings. $NH_4(I)$ experiences hindered rotation
around the polar c axis at room temperature which
persists below Tc. $NH_4(II)$ is disordered with respect
to the plane at $z = \frac{1}{4}$ above Tc and ordered below.
Below Tc, $NH_4(II)$ shows five hydrogen bonds of normal
strength which are responsible for the dielectric
polarization.

X-ray and neutron radiation interact with a crystal
in such a manner that the average position or orientation
of molecules or ions is determined. In contrast,
molecules or ions behave as individuals (in the site
group approximation) with respect to infrared radiation.
Thus, since the potential energy of polyatomic species
composing a crystal is a function of the crystal field,
like species inequivalent with respect to position or
orientation should have different vibrational frequencies.
The infrared spectrum, therefore, provides a convenient
tool for obtaining information supplementary to that
obtained by X-ray and neutron diffraction. The method
becomes greatly more authoritative, of course, if single
crystal spectra taken with polarized radiation are
available.

Crystal Structure and Selection Rules

Ammonium sulfate forms orthorhombic crystals, space group Pna2$_1$ = C_{2v}^9, with four molecules per unit cell (31). The only equipoints available in C_{2v}^9 are general positions the rank of which is four (15, p. 119). Thus, all four sulfate ions in the unit cell may occupy equivalent positions, but the ammonium ions must form two groups or families with four equivalent ions in each family. In the notation of Singh, the two families will be designated $NH_4(I)$ and $NH_4(II)$.

In the exact analysis of crystal spectra (4), like ions inequivalent with respect to position within the unit cell must be treated individually. Figure eight shows the correlation splitting of the normal modes of both $NH_4(I)$ and $NH_4(II)$ as well as for the sulfate ion (all unperturbed ions are tetrahedral). It must be kept in mind that it is only the number of components and not the positions of the components that is predicted by figure eight.

Site group and factor group splitting, which together make up correlation splitting, are represented by the first and second steps, respectively, in figure eight. These sources of splitting have been discussed in an earlier section, but the appearance of multiple components of free ion modes which is due to the existence

of nonequivalent ions within a unit cell has only been
briefly encountered. In the interest of brevity and
convenience in later discussions, the latter splitting
will be called equipoint splitting.

free ion symmetry	site symmetry	factor group symmetry
T_d	C_1	C_{2v}^9

$A_1 : \omega_1$

$E : \omega_2$

$F_1 : $ Rot.

$F_2 : \omega_3, \omega_4, $ Trans.

A

A_1 (IR) (R)

A_2 (R)

B_1 (IR) (R)

B_2 (IR) (R)
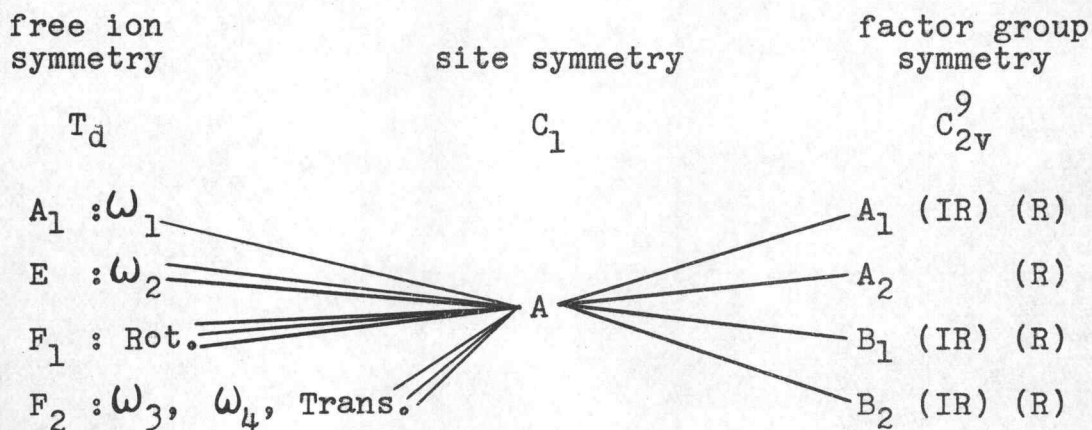
Figure 8. Correlation of symmetry species for
crystalline ammonium sulfate

Thus for each sulfate ion vibration, correlation
splitting predicts $3n$ infrared active components where
n is the degeneracy of the mode. Ammonium ion vibrations
may exhibit $2 \times 3n$ components because of the existence of
two nonequivalent families of ions.

Assignment and Discussion of the Spectra

The general assignment of both ammonium and sulfate
ion vibrations is well known, and so this analysis will
be concerned principally with a discussion of the fine
structure of the bands and changes in the spectrum at
the ferroelectric transition temperature. Figures nine

and ten-a illustrate the spectrum of ammonium sulfate at various temperatures in the frequency ranges 700 to 3800 cm^{-1} and 300 to 700 cm^{-1}, respectively. Individual spectra will be referenced in the text by stating the temperature in degrees Kelvin at which the spectrum was recorded and the figure number.

The Curie temperature of ammonium sulfate is about $223^{\circ}K$; thus spectra 235 and 208 of figure nine were recorded slightly above and below Tc, respectively. Corresponding spectra in the CsBr region are numbered 236 and 208 in figure ten-a. Spectrum 84 figure nine was recorded using liquid nitrogen as the coolant in the cold cell, and 65 figure ten-a was obtained by pumping vigorously on liquid nitrogen. One scan at an even lower temperature was obtained using liquid helium, but unfortunately the actual temperature of the scan is unknown.

The spectra illustrated in figures nine and ten-a were obtained from samples produced by evaporation of aqueous solutions on barium fluoride substrate windows, and the continuous decrease in percent transmission from 1000 to 700 cm^{-1} is due to absorption by the substrate window. The three weak absorptions at 1496, 1592, and 1600 cm^{-1}, which appear in 84 figure nine, result from an unknown impurity introduced during

sample preparation. The observed frequencies of ammonium sulfate and their assignments are listed in table IV.

In table IV, conventional designation has been used for the principal vibrations of ammonium and sulfate ions, and fine structure of the bands has been indexed as follows: components originating from equipoint splitting have been labeled by roman numerals in parenthesis; fine structure attributable to site group splitting has been designated by small case letters; and components which result from factor group splitting have been grouped with brackets.
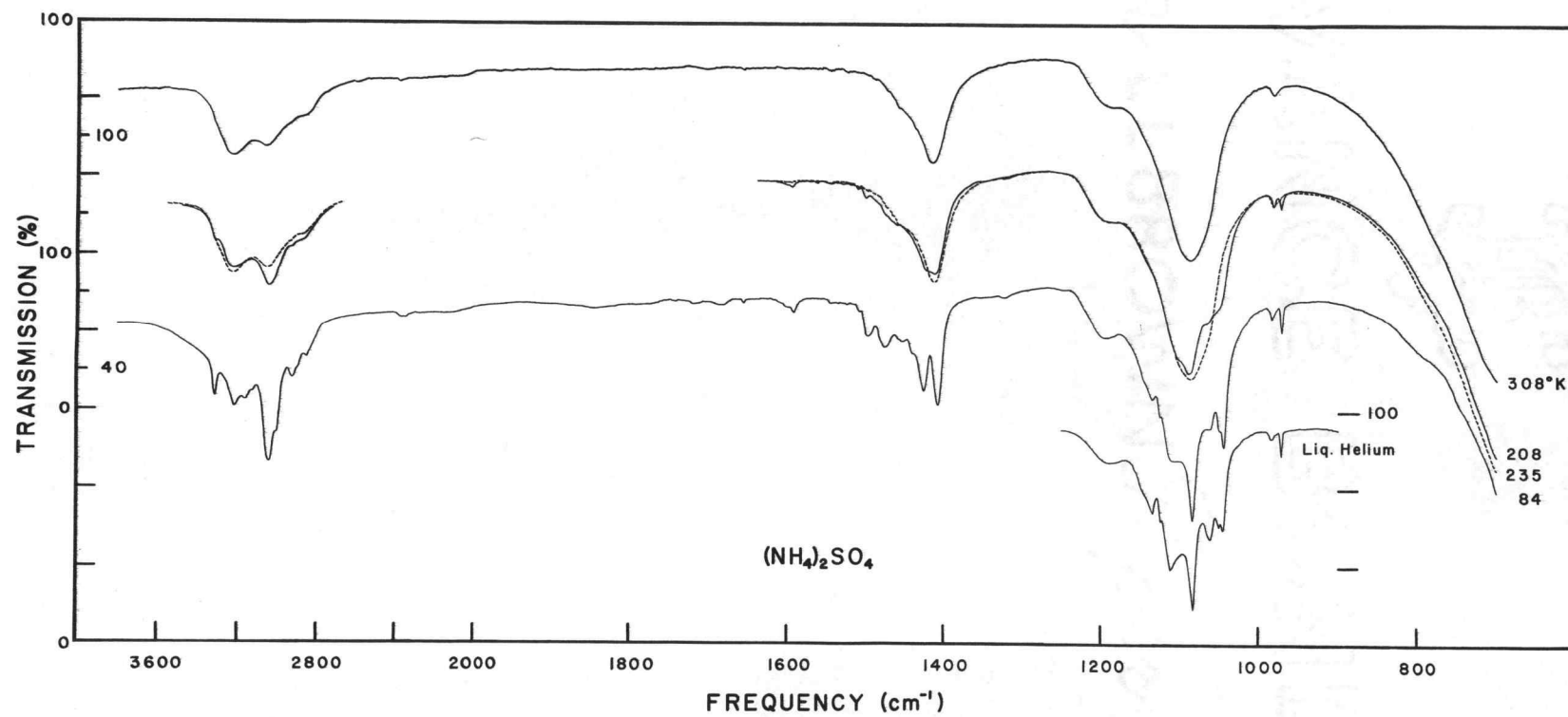
Figure 9. The infrared spectrum of ammonium sulfate from 700 to 3800 cm^{-1}.
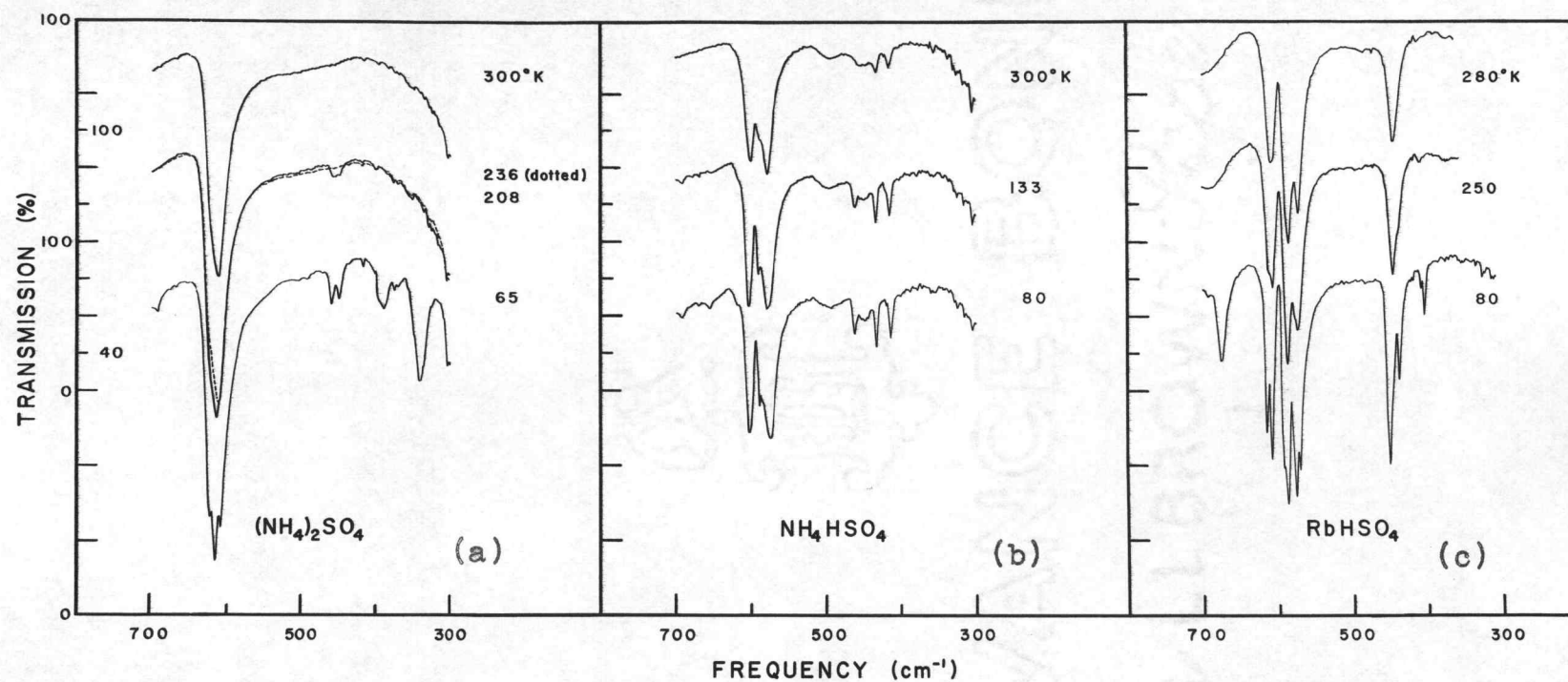
Figure 10. The infrared spectrum of some ferroelectric crystals in the CsBr region: (a) ammonium sulfate, (b) ammonium bisulfate, (c) rubidium bisulfate.

TABLE IV

OBSERVED FREQUENCIES OF CRYSTALLINE AMMONIUM SULFATE

Assignment	C_{2v}^9; 84°K	C_{2v}^9; 308°K	Raman Shifts (1)**
Lattice Modes			72
			181
			193
ω_{Ra}^+	341		
b	375		
c	390		
ω_{2a}^-	450		
	460		449 (8)
b			
ω_{4a}^-	610		
	616	613	621 (8)
b	622		
c			
ω_1^-	[972		
	983	982	978
ω_{3a}^-	[1045		
	[1050		
b	[1061		
	[1084	1086	1091 (54)
c	[1114		
	1126		
	[1135		
$2\omega_4^-$	1195	1190	
$\omega_4^+(I)_a$	1407		
b	1426	1412	
c	1440		
$\omega_4^+(II)_a$	1451		
b	1474		
c	1506		
	1496*		
	1592*		
	1600*		* attributed to impurities
$2\omega_4^+$	2845	2850	
	2923		** frequencies are average values, numbers in brackets are maximum spread of components.
$\omega_3^+(II)_a$	3008		
b	3040	3050	
	3120		
$\omega_3^+(I)_a$	3156		
b	3212	3220	
c	3312		

Ammonium Ions. Singh (31) observed the following:
(1) NH_4(II) was disordered with respect to the plane
$z = \frac{1}{4}$ above Tc and ordered below and showed five hydrogen
bonds of normal strength below Tc which were responsible
for the dielectric polarization, and (2) NH_4(I) under-
went hindered rotation both above and below Tc and as
such did not participate in hydrogen bonding. Thus,
the subject of hydrogen bonding in ammonium sulfate
would appear to be well adapted to infrared study because
of the existence of two nonequivalent families of ammonium
ions only one of which is hydrogen bonded; the salt has,
in effect, a built-in reference or standard. Pimentel
and McClellan (26, p. 167) have enumerated the effects
of hydrogen bonding upon the infrared spectrum. The
most significant effect is to shift stretching vibrations
to lower frequencies, to broaden said vibrations, and
to greatly increase the temperature dependence of their
integrated absorption coefficients.

Aside from the broad band at 2850 cm^{-1} in 308
figure nine, the two absorptions in the high frequency
region of the same spectrum are believed to be stretching
vibrations of the ammonium ions. The lower band at
3050 cm^{-1} must surely be associated with hydrogen
bonded NH_4(II); while 3220 cm^{-1} originates with NH_4(I).
The 3050 cm^{-1} mode shows striking temperature dependence,

which further identifies it with the hydrogen bonded family of ammonium ions. The abrupt increase in intensity of 3050 cm^{-1} at the Curie point is evidence that hydrogen bonded NH_4(II) participates in the ferroelectric transition. At 84°K the lowest stretching frequency is probably 3008 cm^{-1} which corresponds to a hydrogen bond of only intermediate strength.

Bending modes, according to Pimental (26, p. 167), are shifted to higher frequencies by hydrogen bonding, but they suffer no great changes in intensities. Accordingly, in 84 figure nine the trio of lines at 1451, 1474 and 1506 cm^{-1} are assigned to ω_4^+(II); while the trio appearing at slightly lower frequency is assigned to ω_4^+(I). The appearance of three components suggests that only site group splitting (removal of the degeneracy of the F_2 mode) is operative. As in the case of the stretching modes, it is known from experiments in which the infrared intensity at a given wavelength was recorded versus temperature that the components assigned to NH_4(II) appear discontinuously on cooling below Tc.

The first overtone of the bending mode, $2\omega_4^+$, appears at 2850 cm^{-1} in 308 figure nine, and two components, which are assigned to $2\omega_4^+$(I) and $2\omega_4^+$(II), appear in 84 figure nine.

Analogous to the spectrum of ammonium thiocyanate, a librational frequency characterized by restricted rotation around a bond is observed at 341, 375, and 390 cm^{-1} in 65 figure ten-a. This mode is actually a lattice mode of rotary origin. Whether or not it is due to the hydrogen bonded ammonium ion, $NH_4^+(II)$, or to $NH_4^+(I)$, which is known to undergo restricted rotation, is a matter of conjecture. The mode does not appear in the spectrum until well below the Curie temperature, and then its intensity increases continuously with decreasing temperature.

In view of the fact that the E mode of the ammonium ion is not activated in the spectrum of ammonium sulfate, neither of the ammonium ions (I or II) appears to be greatly distorted by the crystal field or by hydrogen bonding. This is not the case with the sulfate ions as discussed in the next section.

Sulfate Ions. Reference to the correlation diagram, figure eight, shows that a triply degenerate, F_2, species of free sulfate ion may produce three components under site group splitting and nine components under factor group splitting. ω_3^-, which is a broad singlet at 1086 cm^{-1} in 308 figure nine, exhibits seven clearly resolved components at low temperatures (the broad band at 1190 cm^{-1} is $2\omega_4^-$); thus it appears that here is an

example of factor group splitting. It is to be noted that the combination mode, $\omega_2^- + \omega_4^-$, would occur at about 1050 cm^{-1}; however none of the rather sharp components in the region of ω_3^- is believed due to this combination for the following reasons: (1) $2\omega_4^-$ is quite broad and weak, and it exhibits no sharp components, and (2) $2\omega_2^-$ does not appear at all.

Further evidence in favor of factor group splitting is the appearance of two clearly resolved components for ω_1^-, the A$_1$ species of free sulfate ion (972 and 983 cm^{-1}). In fact, in the scan at liquid helium temperature a third very weak component of ω_1^- is visible, which is the exact number predicted under factor group selection rules. Of course, another explanation is available which would account for six and two components for ω_3^- and ω_1^-, respectively. If two pairs of equivalent sulfate ions existed instead of the equivalent quartet, then site group splitting plus equipoint splitting would yield the observed spectrum (except for the one extra component of ω_3^-). We do not subscribe to this second explanation, however; since it is not in agreement with the findings of the crystallographers, and it does not predict the observed number of components.

The stretching mode, ω_3^-, shows the most striking

changes at the Curie point. R. Pohlman (27) discovered these changes long ago by plotting the intensity at a given wavelength versus temperature (isochromates). We have duplicated the work at 1051 and 1082 cm^{-1} and obtained excellent agreement. The E mode of sulfate ion, ω_2^-, appears discontinuously at the Curie point on cooling and the change is reversible on heating. Both components of ω_2^- and all three components of ω_4^- are observed in 65 figure ten-a. Thus it appears that stretching modes are more susceptible to factor group splitting than are bending modes.

The abrupt changes at the Curie point in the vibrational modes of both $SO_4^=$ and $NH_4^+(II)$ are evidence that interaction between the two ions is associated with the ferroelectric transition. Furthermore, the temperature behavior of both bending and stretching modes of $NH_4^+(II)$ is typical of hydrogen bonding. Thus it can be concluded with some certainty that dielectric polarization in ammonium sulfate results from the formation of an orientated system of hydrogen bonds NH ---O. Such a network of hydrogen bonds could reasonably produce the crystal field necessary to distort the sulfate ion to the extent indicated by its infrared spectrum.

Rubidium Bisulfate

The relation between the infrared spectrum and the ferroelectric transition of rubidium bisulfate has been investigated by Myasnikova and Yatsenko (21) who also assigned the spectrum. In assigning the spectrum, the perturbing influence of the proton upon the remaining part of the bisulfate ion was not considered; that is, the spectrum was assigned as though the ion has tetrahedral symmetry. This approach led to an assignment for some of the normal modes which is quite different from the assignment proposed here.

The Raman spectrum of bisulfate ion in various environments (molten salt and concentrated solution) has been investigated, and the spectrum has been assigned in each case (30, 38). In general, our assignment of the crystal spectrum is in agreement; however there are differences in detail which will be discussed later. Siebert (30) states that in concentrated sodium bisulfate solution the hydrogen is without noticeable influence on the symmetry of the remaining part of the ion. Since bisulfate ion is less than ten percent dissociated in concentrated aqueous solution at room temperature, the specie observed by Siebert was surely HSO_4^-. But, from this work with crystalline rubidium,

ammonium, and potassium bisulfates, the proton of bisulfate ion is known to have great influence on the symmetry of the remaining part of the ion. The appearance of twelve normal modes is cited as evidence for a C_s structure of bisulfate ion.

Protonation of one oxygen atom of sulfate ion destroys the tetrahedral symmetry, and, because of the nonlinearity of the $S - O' - H$ bond, results in a C_s structure. Nine of the twelve vibrations of bisulfate ion are best determined by stepwise devaluating the symmetry of sulfate ion through the steps C_{3v} and C_s as shown in figure eleven.

T_d, SO_4 (18, p. 151) C_{3v}, OSO_3 C_s, HSO_4

$A_1 : \omega_1$ (981 cm^{-1})

$E : \omega_2$ (451 cm^{-1})

$F_2 : \omega_3$ (1104 cm^{-1})

$F_2 : \omega_4$ (613 cm^{-1})

A_1 ——————— A' (IR)(R)

E ——————— A'' (IR)(R)
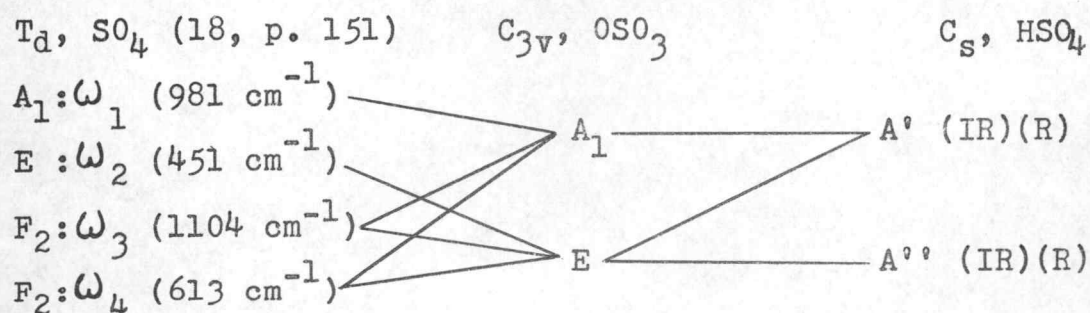
Figure 11. Correlation of bisulfate ion species which are associated with sulfur and oxygen atoms.

The remaining three vibrations are associated with the proton; two vibrations, a bending mode and a stretching mode, are A' (symmetric with respect to the plane of symmetry), and one, an out of plane bending mode, is A''. Thus, the bisulfate ion should have a total of eight A' and four A'' vibrations, all of which are permitted infrared activity.

A further aid to understanding the spectrum is that, unless the influence of the proton is exceptionally large, normal modes of bisulfate ion which have the same origin in figure 11 should lie in close proximity in the bisulfate ion spectrum. According to Siebert (30), ω_3^- of sulfate ion (1104 cm^{-1}) can be traced to two main components, 1200 and 1040 cm^{-1}, for bisulfate ion which correspond to E and A_1 species, respectively, in the C_{3v} approximation. The totally symmetric stretching vibration of sulfate ion (981 cm^{-1}) can be traced to SO' stretching in bisulfate ion, where O' is the protonated oxygen atom. Protonation of O' causes a softening of the SO' bond and an increase in the effective mass of O'. Both of these effects contribute to shift SO' stretching to lower frequency.

Crystal Structure and Selection Rules

The crystal structure of rubidium bisulfate has recently been redetermined (24). Above -15°C, the Curie

point, the symmetry was found to be monoclinic,
$P_C^2 1 = C_{2h}^5$, with lattice constants $a_o = 14.35$, $b_o = 4.62$,
$c_o = 14.81$, and $\beta = 121.0^o$. All distances were
given in angstrom units. Below Tc the two fold screw
axis disappeared, and the space group became Pc = C_s^2.
In both allotropic forms there are eight molecules per
unit cell.

Considering the nonferroelectric phase first, the
equipoints available in C_{2h}^5 have the trivial symmetry;
thus all ions must occupy general positions. General
positions of C_{2h}^5 have rank four; therefore to
accomodate eight molecules per unit cell, two non-
equivalent equipoints must be occupied which give rise
to two nonequivalent families of both bisulfate and
rubidium ions with four ions per family. Rubidium ions
will not be considered further, because the frequencies
involving them, lattice modes, were not observed in this
work. The existence of two nonequivalent families of
bisulfate ions may produce a doublet splitting of each
normal mode of the free ion which will again be referred
to as equipoint splitting. In addition, doublet
splitting of every mode of the free ion is predicted by
the correlation chart in figure twelve; the latter
splitting is, of course, factor group splitting.

Below the Curie point, the crystal structure

becomes C_s^2 with yet eight molecules per unit cell.
Loss of the two fold screw axis at Tc reduces the rank
of C_1 equipoints to two. The eight bisulfate ions per
unit cell are thus forced to form four families of
ions with two ions per family. This fact predicts four
components (equipoint splitting) for each vibrational
mode of the free ion even before considering site and
factor group effects. Figure twelve predicts an
additional doublet, factor group splitting, for each
component.

It is interesting to note that the Raman and
infrared frequencies may not coincide above the Curie
point; whereas they must be identical below.

free ion symmetry	site symmetry	factor group symmetry
C_s	C_1	C_{2h}^5

Ag   (R)
Bg   (R)

Au   (IR)
Bu   (IR)

A'
A''   A

C_s^2

A'   (IR)(R)
A''   (IR)(R)
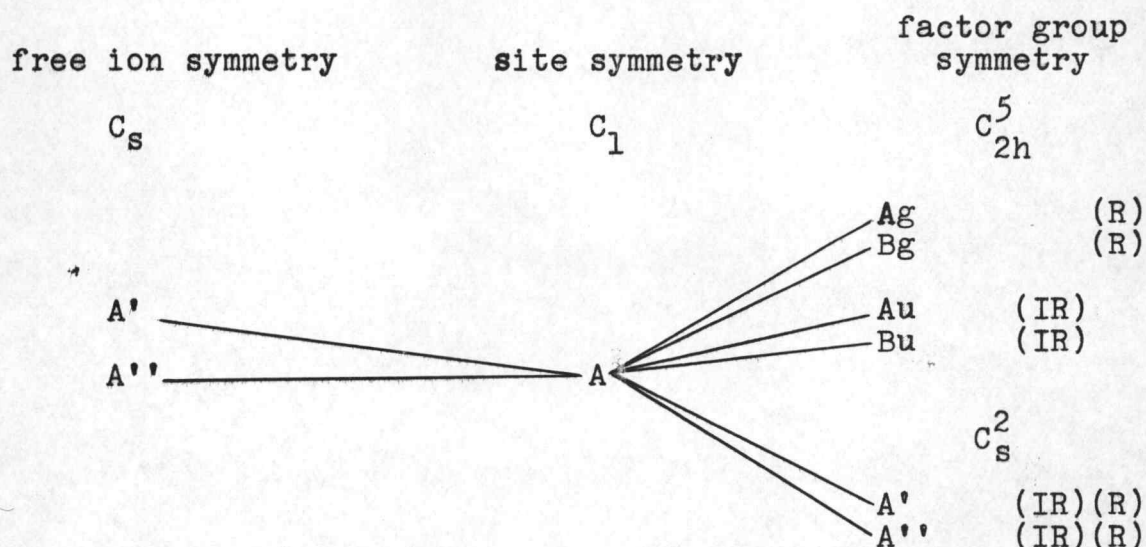
Figure 12. Correlation of symmetry species
for crystalline rubidium bisulfate

Assignment and Discussion of the Spectra

Figure thirteen shows the infrared spectrum of rubidium bisulfate and its deuterated analog in the frequency range 700 to 3600 cm^{-1}. The spectrum of rubidium deuterobisulfate will not receive individual treatment, but will be discussed in relation to the bisulfate spectrum.

The spectra from 700 to 3600 cm^{-1}, as illustrated, were obtained from samples produced by evaporation of aqueous rubidium bisulfate solutions on barium fluoride substrate windows. The following characteristics of the spectra are attributable to the substrate window or to impurities introduced during sample preparation: (1) continuous decrease in percent transmission from 1000 to 700 cm^{-1} (2) the appearance of absorptions at 975, 1072, and 1110 cm^{-1} which are due to sulfate ion, and (3) absorptions at 1350, 1500, and 1600 cm^{-1} which have unknown origin. The disturbance on either side of 2350 cm^{-1} results from atmospheric carbon dioxide. Rubidium bisulfate and deuterobisulfate spectra were recorded from nujol mulls and fluorolube mulls as well as from samples produced by solvent evaporation. The frequencies listed in table five appear consistently in all spectra, and hence they are believed to be real sample vibrations. Spectra in the low frequency range,

figure 10-c, were recorded from nujol mull samples only.

Two sources of doublet splitting are operative in the paraelectric phase. These are equipoint splitting and factor group splitting. Equipoint splitting depends upon the relative unbalance of the crystal field at the positions of like but inequivalent ions, whereas the criteria for factor group splitting may be simply (1) the distance of separation of equivalent ions, (2) the number of foreign ions interposed between equivalent ions, and (3) the actual number of equivalent ions per unit cell. In the spectrum under consideration, simply counting components is sufficient to differentiate between the two types of splitting and prove that equipoint and not factor group splitting is responsible for multiple components in the spectrum. Table V lists the observed frequencies and their assignments.

Indexing the vibrations presented a problem because of the existence of a very large number of normal modes most of which have multiple components. It was decided that less confusion would result if bisulfate ion vibrations which are derived from sulfate ion vibrations were designated by the conventional symbol for the sulfate mode, followed in parenthesis by the symmetry species in the C_{3v} approximation and the actual symmetry species for the free bisulfate ion. Vibrations which have their origin in the proton of bisulfate ion are labeled with a

lower case letter (s = stretching, b = bending) followed
in parenthesis by the actual symmetry species. Components
arising from equipoint splitting are designated by
appending a roman numeral to the symbol.
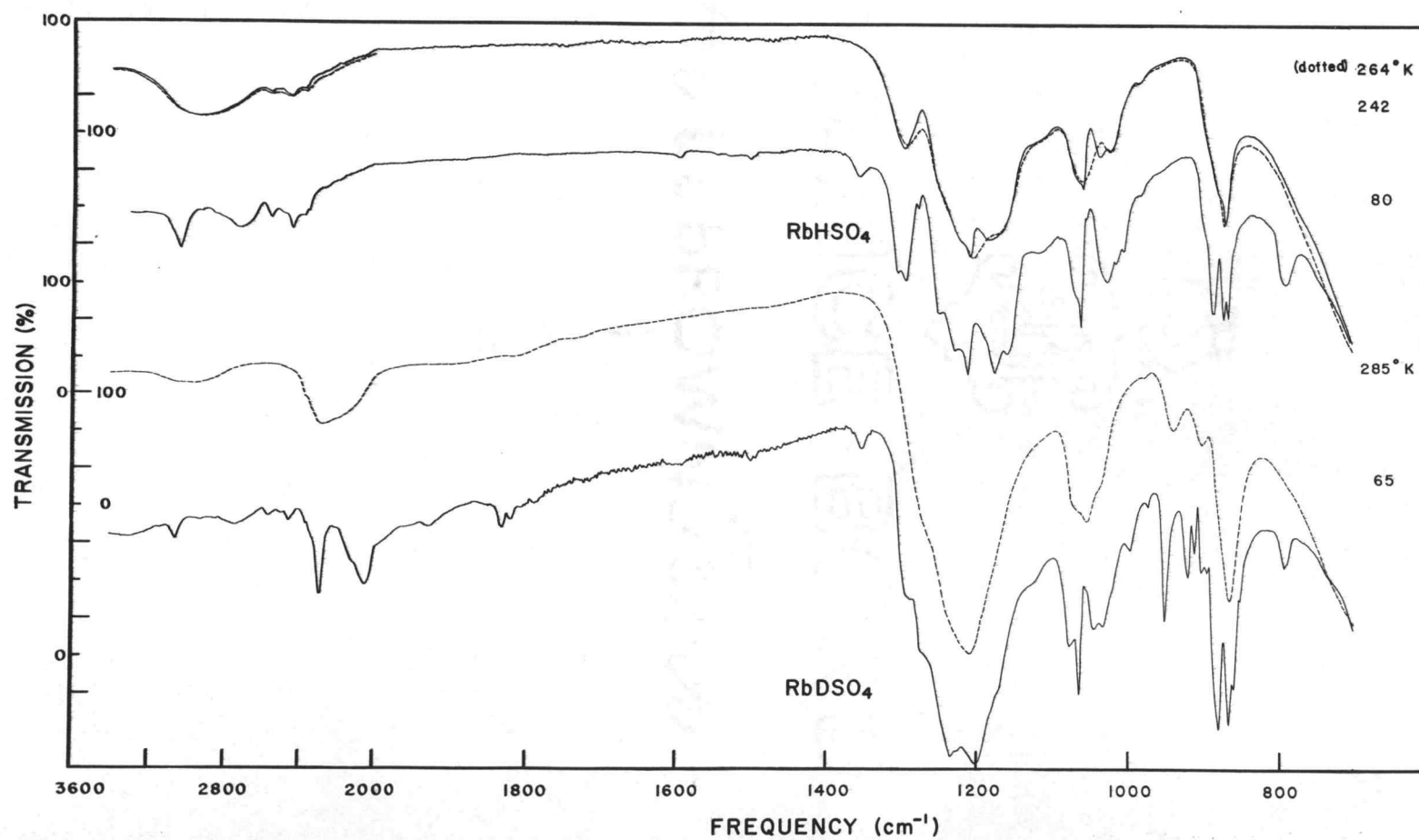
Figure 13. The infrared spectrum of rubidium bisulfate from 700 to 3600 cm^{-1}.

68

TABLE V

OBSERVED FREQUENCIES OF CRYSTALLINE RUBIDIUM BISULFATE

Assignment		$RbHSO_4$		$RbDSO_4$	
		C_s^2; 80°K	C_{2h}^5; 264°K	C_s^2; 65°K	C_{2h}^5; 285°K
				385	
$\omega_2^-(E,A")$	I	405		402	401
	II	410		407	
$\omega_2^-(E,A')$	I	438	446	428	436
	II	450		440	
$\omega_4^-(E,A')$	I	570	573	567	567
	II	575		575	573
$\omega_4^-(E,A")$	I	585	587	585	584
	II	590			
$\omega_4^-(A_1,A')$	I	606	609	606	606
	II	612		612	
$\omega_b^-(A")$	I	675		504	
	II	790		530	515
	III	797			
$\omega_1^-(A_1,A')$	I	860		852	
	II	866		860	
	III	874	870	866	865
	IV	885		874	
		900		895	
		975*	975*	975*	975*
$\omega_3^-(A_1,A')$	I	1005		998	
	II	1013	1020	1033	1035
	III	1036		1045	
		1055		1055	1055
	IV	1063	1060	1065	
		1072*		1076*	1072*
		1110*			
$\omega_3^-(E,A")$	I	1158			
	II	1175	1170	1170	
$\omega_3^-(E,A')$	I	1212	1205	1200	1200
	II	1228	1220	1235	
$\omega_b^-(A')$	I	1250	1245	903	904
	II	1275		913	
	III	1292	1292	921	941
	IV	1304		952	
		1350*			
		1500*			
		1600*			
$2\omega_b^-(A')$		2440	2450	1780	1805
		2485		1825	
		2560	2560	1920	1880
$\omega_s^-(A')$	I	2700		2040	
	II	3040	2940	2290	2265

*attributed to impurities

<u>Vibrations of the OH Group</u>. Rubidium bisulfate is strongly hydrogen bonded as evidenced by the position of the OH stretching mode, 2940 cm^{-1} in spectrum 264 figure 13, and its behavior with temperature. The very weak pair of lines at 2560 and 2450 cm^{-1} in the same spectrum are known to be OH vibrations also, because they have counterparts at 1880 and 1805 cm^{-1} on deuteration. However, it is not known with assurity whether they are stretching vibrations or overtones of the OH in plane bending vibration, $\omega_b(A')$, which has two components, 1292 and 1245 cm^{-1}. The 1245 cm^{-1} component is nearly obscured by the neighboring very strong SO vibration, but it is known to exist because its counterpart on deuteration appears at 904 cm^{-1} in spectrum 285 figure 13. Because of the excellent correspondence of the 2560 and 2450 cm^{-1} modes with the calculated overtone frequencies, 2584 and 2490 cm^{-1}, the absence of temperature dependence, and their small intensities, the overtone assignment is preferred. If this is the true assignment, then only the broad band at 2940 cm^{-1} in the stretching region can be assigned to $\omega_s(A')$. Thus neither equipoint nor factor group splitting is operative above the Curie point to the extent necessary to produce a resolvable separation of components.

Below the Curie temperature a quadruplet equipoint

splitting of each mode of the free ion is predicted, and an additional doublet splitting is possible which arises from factor group splitting. Spectra 264 and 242 of figure 13 were recorded at temperatures which bracketed the Curie point, $(258^{\circ}K)$; and it can be seen that no large or discontinuous changes in the infrared spectrum accompany the ferroelectric transition. This is in harmony with the findings of Pepinsky (24) who concluded that the transition was second order. On decreasing the temperature below the Curie point, a separation of the 2940 cm^{-1} mode into two components occurs continuously over a wide temperature interval. At $80^{\circ}K$ only two components, 3040 and 2700 cm^{-1}, instead of the predicted quadruplet, are apparent.

The OH in-plane bending fundamental, $\omega_b(A')$, shows four clearly resolved components at $80^{\circ}K$, and this is strong evidence for the existence of four nonequivalent pairs of bisulfate ions in the ferroelectric phase. It is probable that no examples of factor group splitting have been observed for the OH vibrations.

The OH out-of-plane bending fundamental, $\omega_b(A'')$, was observed only in the low temperature spectrum. Three of its four possible components were found in the $RbHSO_4$ spectrum; whereas all four components were found for $RbDSO_4$. The doublet at 797 and 790 cm^{-1} and the single

line at 675 cm^{-1} in the RbHSO$_4$ spectrum recorded at
80°K were assigned to $\omega_b(A'')$. The counterparts of
the 797 and 790 cm^{-1} modes produced by deuteration
occur at about 590 cm^{-1} and may be partly responsible
for the abnormal intensity of the SO bending mode at
the same frequency. The 675 cm^{-1} mode is shifted to
504 cm^{-1}, and the fourth component of $\omega_b(A'')$ appears
at 530 cm^{-1} in the spectrum of RbDSO$_4$ recorded at 65°K.

Vibrations of the OSO$_3$ Group. Figure 11 and the
data of Siebert (30) are the bases for assigning the
SO stretching vibrations. The A$_1$ mode of sulfate ion
(981 cm^{-1}) should occur at lower frequency for
bisulfate ion. This mode consists primarily of S - O'
stretching, where O' is the protonated oxygen of
bisulfate ion, and hence should exhibit a small shift
to lower frequency on substituting deuterium for hydrogen.
The 870 cm^{-1} mode in 264 figure 13 satisfies both above
requirements and is assigned to the symmetric S - O'
stretching vibration, $\omega_1(A_1,A')$. At low temperature
this mode splits into four components, and we believe
this to be additional direct evidence for the existence
of four nonequivalent bisulfate ions per unit cell in
the ferroelectric phase.

The A$_1$ and E modes of the C$_{3v}$ model, which correlate
with the F$_2$ species of sulfate ion in figure 11, occur

as the 1060 - 1020 cm^{-1} doublet and 1205 cm^{-1} modes, respectively, in 264 figure 13. At low temperature the 1205 cm^{-1} mode splits into two well resolved doublets which are assigned to A' and A" species of C_s which correlate with E of C_{3v}. The A_1 mode of C_{3v} occurs in a region that is complicated by the F_2 vibration of sulfate ion impurity, and the relative intensity of the 1063 cm^{-1} line is greatly enhanced by the superimposed impurity mode.

The remaining OSO_3 vibrations, which are all bending modes, suffer only slight displacements from the modes of sulfate ion with which they correlate, and hence they are very easily assigned. Equipoint splitting of the bending modes is effective in producing only doublet splitting instead of the possible quadruplet. This is reasonable since the stretching modes of OSO_3, and even the OH stretching and bending vibrations, all exhibit two main components.

The relation between ferroelectricity of rubidium bisulfate and hydrogen bonding is not well defined by the infrared spectrum, because the transition is second order and occurs at high temperature. Nevertheless, the two are believed related because of the following: (1) the vibrations most affected by hydrogen bonding (SO' stretching and OH bending and stretching) exhibit great changes on cooling below Tc, (2) changes in SO'

stretching and OH bending actually begin at Tc.

The spectrum at liquid nitrogen temperature clearly proves that in the ferroelectric phase eight bisulfate ions per unit cell form four families with two ions per family. However, the principal splitting is only a doublet; therefore the families are related in pairs. This is the relation expected if the ferroelectric crystal symmetry is formed by a small perturbation of the high temperature structure.

Ammonium Bisulfate

Since the discovery of ferroelectricity in ammonium bisulfate by Pepinsky et al. in 1958 (25), the infrared spectrum has been investigated with respect to the ferroelectric transition by Myasnikova and Yatsenko (21). They assigned the bisulfate ion spectrum on the basis of a tetrahedral structure, an assumption with which this work is contradictory; but they concluded that ferroelectricity resulted from hydrogen bonds, O---HO, which appears to be a valid conclusion.

Ammonium bisulfate is one of the few compounds that exhibits ferroelectricity within a temperature interval; that is, it has an upper and a lower Curie point. The upper Curie point, $-3^{\circ}C$, is associated with a second order transition, and the lower transition, $-119^{\circ}C$, is first order (25).

Crystal Structure and Selection Rules

Above $-3^{\circ}C$, $270^{\circ}K$, the structure of ammonium bisulfate is monoclinic, $P_c^{2}1 = C_{2h}^5$ with lattice constants: $a_o = 14.51$, $b_o = 4.54$, $c_o = 14.90$, and $\beta = 120^{\circ} 18'$. Between $270^{\circ}K$ and $154^{\circ}K$ the substance is ferroelectric, and its structure is monoclinic, $Pc = C_s^2$. At $243^{\circ}K$ the lattice constants are $a_o = 14.26$, $b_o = 4.62$, $c_o = 14.80$, and $\beta = 121^{\circ} 18'$. Loss of the

glide plane on cooling below $154^{\circ}K$ results in a triclinic structure, $P1 = C_1^1$, which at $133^{\circ}K$ has lattice constants; $a_o = 14.24$, $b_o = 4.56$, $c_o = 15.15$, $\alpha = 90^{\circ}$, $\beta = 123^{\circ} \, 24'$, and $\gamma = 90^{\circ}$. All distances are given in angstrom units, and there are eight molecules per unit cell in all structures, (25).

Both ammonium and bisulfate ions occupy general positions in all three crystal structures. The rank of C_1 equipoints of C_{2h}^5, C_s^2, and C_1^1 is four, two, and one respectively; thus, with eight molecules per unit cell, equipoint splitting may produce respectively a doublet, a quartet, and eight components of each mode of the free ion. With respect to the crystal structure data, it should be noticed that (1) the crystal symmetries obtained by cooling are subgroups of the symmetry of the phase stable at the next higher temperature (that is to say, C_s^2 is a subgroup of C_{2h}^5 and C_1^1 is a subgroup of C_s^2), and (2) the lattice constants suffer no great changes on passing from the most symmetric to the least symmetric phase. Thus one would expect that the principal splitting due to inequivalence of position would be a doublet splitting (predicted for C_{2h}^5) and that splitting attributable to lower crystal symmetries would appear as perturbations and be small with respect to the original doublet separation.

The symmetry, normal modes, and vibrational
frequencies of both free ammonium and bisulfate ions
have been discussed in previous sections. Figure 14
correlates the symmetry species of the free ions with
site group and factor group symmetries applicable to
the three known structures of ammonium bisulfate.
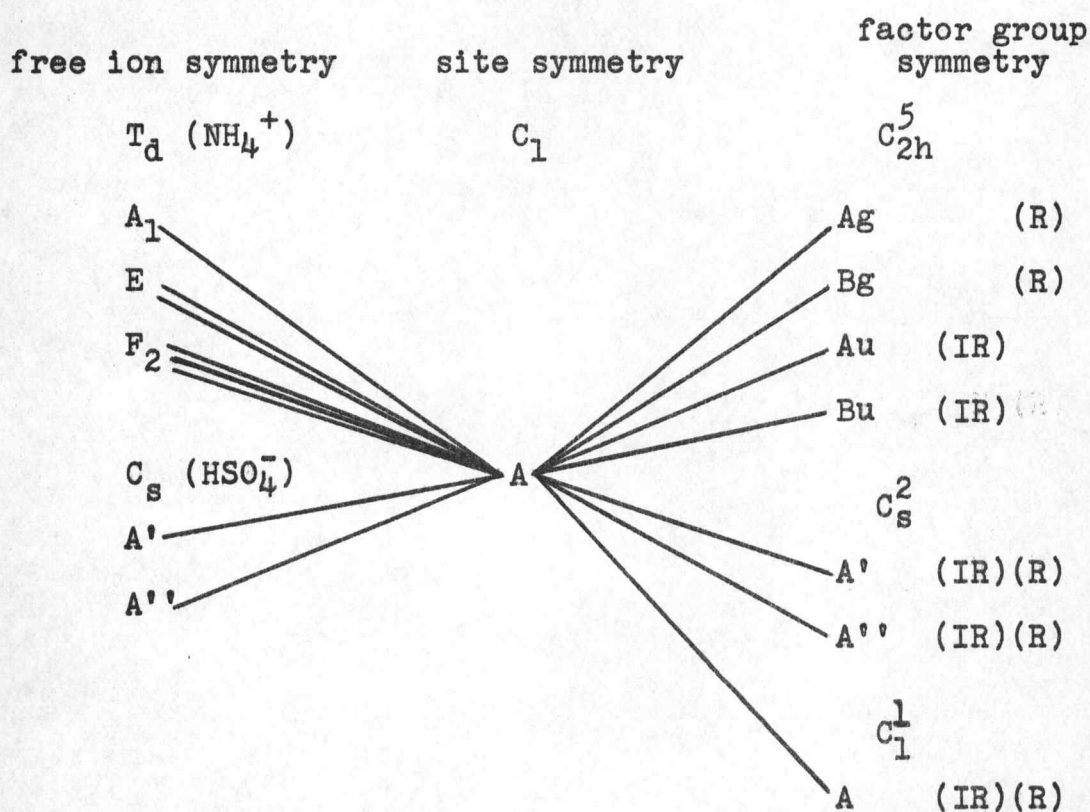
Figure 14. Correlation of symmetry species for
crystalline ammonium bisulfate

From figure 14 it is seen that the perturbation of completely asymmetric surroundings may remove all degeneracies, site group splitting; and coupling of like vibrational modes of equivalent ions within the unit cell may result in an infrared active doublet for each component in both room temperature and ferroelectric phases. The frequencies observed in the infrared should be identical to the Raman shifts in both the ferro-electric and lower temperature phases, whereas they may not be identical above the upper Curie point.

As stated before, site group and equipoint splitting depend upon the crystal field, and as yet their magnitudes are not predictable beyond a qualitative estimate. For certain vibrations, merely counting components will suffice as a criterion for differentia-tion; whereas for other modes, one can only use intuition. An empirical observation in this work has been that site group splitting appears first followed by what has been called equipoint splitting, and factor group splitting is the smallest effect.

The infrared spectrum of ammonium bisulfate is illustrated at various temperatures in figures 10-b and 15. Figure 10-b includes the $CsBr$ region, and figure 15 shows the spectrum from 700 to 3800 cm^{-1}.
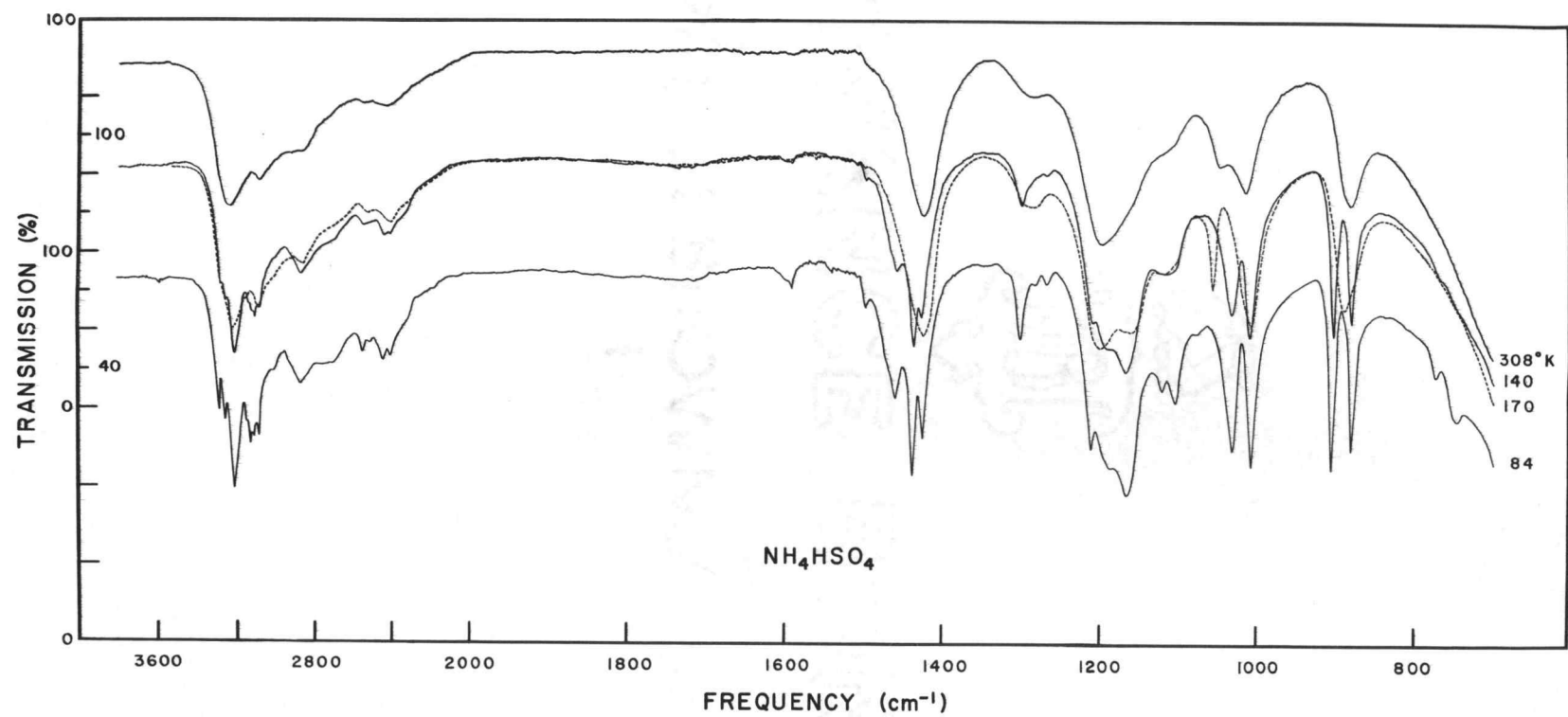
Figure 15. The infrared spectrum of ammonium bisulfate from 700 to 3800 cm⁻¹.

Assignment and Discussion of the Spectra

All of the spectra of ammonium bisulfate illustrated
in figure 15 were recorded from samples produced by
evaporation of aqueous solutions on barium fluoride
substrate windows. The decrease in percent trans-
mission in the frequency range 1000 to 700 cm^{-1} is due
to absorption by the substrate, and the maxima occuring
at 1080, 1495, 1592, and 1600 cm^{-1} are due either to
sulfate ion impurity, which was produced by interaction
of sample and substrate during sample preparation, or
to some other unknown impurity, also introduced during
sample preparation.

Ammonium bisulfate was studied also as the nujol
and fluorolube mull. The spectra in figure 10-b are
actually the nujol mull scans. As in the case of the
previous two ferroelectric compounds, mull spectra in
the high frequency region did not have the detail
shown by the spectra of samples produced by solvent
evaporation. The frequencies listed in table six
appeared in all spectra having sufficient detail, and
hence they are believed to belong to crystalline ammonium
bisulfate. The nomenclature for ammonium and bisulfate
ion vibrations has been discussed in previous sections
dealing with ammonium sulfate and rubidium bisulfate
respectively.

TABLE VI

OBSERVED FREQUENCIES OF CRYSTALLINE AMMONIUM BISULFATE

Assignment		c_1^1, 84°K	c_s^2, 170°K	c_{2h}^5, 308°K
$\omega_2^-(E,A'')$	I	415	414	415
	II	433	431	431
$\omega_2^-(E,A')$	I	449	446	
	II	462	458	450
$\omega_4^-(E,A')$		574	577	578
(E,A'')		590	589	588
(A_1A')		602	600	600
$\omega_b^-(A'')$	I	748		
	II	775		
$\omega_1^-(A_1,A')$	I	882	890	880
	II	906		
$\omega_3^-(A_1,A')$	I	1009	1008	1015
	II	1032	1057	1045
		1080*		
$\omega_3^-(E,A'')$	I	1104		
	II	1122	1120	1120
$\omega_3^-(E,A')$	I	1166	1162	
	II	1186	1200	1197
$\omega_b^-(A')$	I	1212		
	II	1268		
	III	1282		
	IV	1302	1285	1285
ω_4^+	a	1425		
	b	1438	1424	1422
	c	1460		
		1495*		
		1592*		
		1600*		
$2\omega_b^-(A')$		2412		
		2450	2410	2430
		2510		
		2555	2530	2550
$\omega_s^-(A')$		2700		
$2\omega_4^+$		2875	2865	2900
ω_3^+; ω_1^+ and		3010		
		3084	3096	3094
$\omega_s^-(A')$		3110		
		3124		
		3136		
		3206		
		3254	3220	3240
		3282		

*attributed to impurities

Ammonium Ions. Since both ammonium and bisulfate ions have been encountered previously, only a rather brief discussion is called for.

The E mode of ammonium ion does not appear in the spectrum (1670 cm^{-1} for ammonium thiocyanate), and hence the tetrahedral symmetry of ammonium ions in the crystal is not drastically perturbed. The A_1 mode, which is not allowed for the tetrahedral structure, then likely appears only at low temperatures, if at all. On this basis, six of the group of eight lines from 3010 to 3282 cm^{-1} of spectrum 84 figure 15 are assigned to ω_3^+. The weak shoulder which appears in the low temperature spectrum at 3010 cm^{-1} may well be ω_1^+. With six components in the low temperature spectrum, the degeneracy of the F_2 species is known to be broken, and equipoint splitting is operating to produce a doublet of each component. The eighth component of the group of lines likely belongs to OH stretching of the bisulfate ion. The corresponding mode for rubidium bisulfate occured at 3040 cm^{-1}, but any definite assignment in the ammonium bisulfate spectrum seems presumptive.

The bending mode of ammonium ion, ω_4^+, appears with three components, the number predicted by site group splitting. The first overtone of ω_4^+ also appears strongly at 2875 cm^{-1} in the spectra of all three phases.

In figure 10-b, which illustrates the low frequency spectrum of ammonium bisulfate, attention should be called to the fact that no torsional modes of ammonium ion appear (contrasted to ammonium sulfate and ammonium thiocyanate where two or perhaps three components appear).

There are two possible types of hydrogen bonds in NH_4HSO_4, NH --- O and O'H --- O. No evidence for the existence of the former type is found in the spectra (compare with figure nine wherein ω_4^+ for hydrogen-bonded ammonium ions is illustrated). The latter type of interaction is discussed in the following section.

Bisulfate Ions. At liquid nitrogen temperature, vibrational frequencies associated with the hydroxyl group of bisulfate ion are remarkably similar to corresponding vibrations of rubidium bisulfate. On the basis of relative intensity changes produced by deuteration, the line at 1212 cm^{-1} in spectra 140 and 84 figure 15 is included in the OH bending frequencies, $\omega_b(A')$. Since bending modes are shifted to higher frequencies by hydrogen bonding, it appears that a quartet of bisulfate ions in the low temperature phase is only very weakly hydrogen bonded (compare with the corresponding mode for the rubidium salt which appears at 1250 cm^{-1}).

It is to be noted that no great changes in the ammonium bisulfate spectrum appear at the upper Curie point (second order transition), and the only appreciable change

in the spectrum produced by cooling to $154°K$ is a contin-
uous shift and slight sharpening of some vibrations. The
lower Curie point is associated with a first order
transition, and the spectrum suffers numerous large and
discontinuous changes which are also reversible on heating.
Both isochromates at selected frequencies and repeditive
scans of various frequency regions were made to verify
that the spectrum changed discontinuously at the lower
Curie point. It is to be noted that the lines at 906 and
$1032 \ cm^{-1}$ appeared abruptly at Tc. It might be inferred
from figure 15 that $1057 \ cm^{-1}$ of 170 shifted to $1032 \ cm^{-1}$
of 84, but such is not the case. The mode at $1057 \ cm^{-1}$
appeared at Tc and $1032 \ cm^{-1}$ disappeared.

It seems also that the prediction made earlier in the
section that equipoint splitting would most probably
produce a doublet separation is correct. Bisulfate ion,
being more polarizable than ammonium ion, exhibits the
effect to the greater extent; although ammonium ion
stretching vibrations do exhibit structure which must be
attributed to equipoint splitting.

The relation between hydrogen bonding and ferro-
electricity in ammonium bisulfate is not at all clear from
the infrared spectrum. Within the ferroelectric temper-
ature region, the SO' stretching and OH stretching and
bending vibrations show but single components. The
vibrations should be split, as with rubidium bisulfate, if

the eight bisulfate ions per unit cell were divided into
four families which differ with respect to site symmetry
and hence interionic interaction. There is little evidence
of hydrogen bonding in the ferroelectric phase. However,
such evidence would not be easily identified, because no
absolute reference is available. A network of rather weak
bonds could exist and not be apparent in the spectrum.
Actually the existence of a set of weak hydrogen bonds is
in harmony with the findings of Pepinsky et al. (25) who
found ammonium bisulfate to have a very low coercive field.

Ammonium and rubidium bisulfates are isomorphous both
above and within their respective ferroelectric regions,
but their spectra do not exhibit gross similarity until
the ammonium salt transforms to a nonferroelectric phase
at -119°C. However, it is believed that in both salts
dielectric polarization results from an oriented network
of hydrogen bonds and that the differences in the spectra
are due simply to a difference in the relative strength of
hydrogen bonds. Indeed, this belief is supported by the
relative magnitudes of the coercive fields of the two
salts.

Summary

$(NH_4)_2SO_4$, $RbHSO_4$, NH_4HSO_4, and their deuterderiva-
tives were studied with respect to their ferroelectric
transitions and low temperature spectra. Samples
were produced by evaporation of aqueous solutions upon
insoluble BaF_2 substrate windows and by mulling with
nujol or fluorolube.

The spectra at low temperature were quite complex;
the observed multiplicity was assigned on the following
bases (1) equipoint splitting which originates in the
exact theory of crystal spectra whenever like ions
occupy inequivalent positions on the crystal lattice,
(2) site group splitting which may arise for degenerate
modes of free ions whenever the site symmetry is less
than the point symmetry of the free ion, and (3) factor
group splitting which is produced by coupling of like
vibrational modes among equivalent ions within a unit
cell of the crystal. Often the number of components and
their relative positions were sufficient to differentiate
among the three sources of multiplicity. It was found
that site group splitting was the dominant effect
followed by equipoint and factor group splitting in that
order.

Ammonium sulfate suffers a first order transition

at $-49^{\circ}C$, and at that temperature its spectrum exhibits
marked and reproducible changes which are reversible
with temperature inversion. Two nonequivalent families
of ammonium ions are indicated by the spectrum (equipoint
splitting), and the triply degenerate stretching mode
of sulfate ion exhibits site and factor group splitting.
This is the only unequivocable example of factor group
splitting observed in this investigation. The position
and temperature dependence of ammonium ion stretching
modes proves that one family of ammonium ions is
hydrogen bonded in the ferroelectric phase, and this
may very well be the source of dielectric polarization.

Rubidium bisulfate undergoes a second order
transition at $-15^{\circ}C$, but its spectrum shows little change
at that temperature. Further cooling produces continuous
changes in the spectrum and the revelation of fine
structure predicted by equipoint splitting. The observed
spectra are consistent with a C_s structure for bisulfate
ion. Hydrogen bonding definitely exists in the ferro-
electric phase; and, as for ammonium sulfate, may well
be the cause of ferroelectricity.

Ammonium bisulfate exhibits two transformations
between room and liquid nitrogen temperature. The
upper Curie point, $-3^{\circ}C$, is second order, and the
spectrum is completely indifferent to that temperature.

Between $-3^{o}C$ and $-119^{o}C$ the substance is ferroelectric, but the spectrum shows no features that can be attributed to the effect. The lower transformation is first order, and the spectrum shows some remarkable changes at the transformation temperature. Ammonium and rubidium bisulfates are isomorphous both above and within their ferroelectric regions, but it is not until the ammonium salt undergoes the transformation to produce a non-ferroelectric phase $(-119^{o}C)$ that their spectra exhibit great similarity. Yet, it was concluded that ferroelectricity resulted from the existence of a network of hydrogen bonds and that differences in the infrared spectra of rubidium and ammonium bisulfates were simply due to differences in the relative magnitudes of hydrogen bonding.

VI. BIBLIOGRAPHY

1. Ananthanarayanan, V. A comparitive study of the Raman spectra of anhydrous sulphates and estimation of crystalline forces. Indian Journal of Pure and Applied Physics 1: 58-61. 1963.

2. Beckman Instruments. Cesium iodide long wavelength interchange and filter assembly for IR-7 spectrophotometers. Fullerton, California. Beckman Instruments Inc. 1961. 11 p.

3. Beckman Instruments Inc. IR-7 infrared spectrophotometer instruction manual. Fullerton, California. Beckman Instruments Inc. 1960. 85 p.

4. Bhagavantam, S. and T. Venkatarayudu. Raman effect in relation to crystal structure. Proceedings of the Indian Academy of Science 9A: 224-258. 1939.

5. Couture-Mathieu, Lucienne. et al. Dielectric anomalies of ammonium sulfate. Comptes Rendus des Séances de l'Académie des Sciences 242: 1804-1806. 1956.

6. Decius, J.C. Compliance matrix and molecular vibrations. Journal of Chemical Physics 38: 241-248. 1963.

7. Dows, David A. Vibrational spectra of crystalline methyl halides. Journal of Chemical Physics 29: 484-489. 1958.

8. Dows, David A., Eric Whittle, and George C. Pimentel. Infrared spectrum of solid ammonium azide: A vibrational assignment. Journal of Chemical Physics 23: 1475-1479. 1955.

9. Guillien, M. Robert. Sur la constante diélectrique du sulfate d'ammonium au voisinage du point λ. Comptes Rendus des Séances de l'Académie des Sciences 208: 980-981. 1939.

10. Halford, Ralph S. Motions of molecules in condensed systems: I. Selection rules, relative intensities, and orientation effects for Raman and infrared spectra. Journal of Chemical Physics 14: 8-15. 1946.

11. Herzberg, Gerhard. Molecular spectra and molecular structure II. Infrared and Raman spectra of polyatomic molecules. 10th printing. New York. VanNostrand. 1962. 632 p.

12. Hexter, R.M. Relative magnitude of crystal fields; crystal structure of methyl iodide. Journal of Chemical Physics 25: 1286. 1956.

13. Hornig, Donald F. The vibrational spectra of molecules and complex ions in crystals: I. General theory. Journal of Chemical Physics 16: 1063-1076. 1948.

14. Hoshino, S. et al. Dielectric and thermal study of $(NH_4)_2SO_4$ and $(NH_4)_2BeF_4$ transitions. Physical Review 112: 405-412. 1958.

15. International Union of Crystallography. International tables for X-ray crystallography Vol. 1. Kynoch Press, Birmingham, England. 1952. 558 p.

16. Jones, Llewellyn H. Infrared spectrum and structure of thiocyanate ion. Journal of Chemical Physics 25: 1069-1072. 1956.

17. ———————— Polarized infrared spectrum of potassium thiocyanate. Journal of Chemical Physics 28: 1234-1236. 1958.

18. Kohlrausch, K.W.F. Ramanspektren Akademische Verlagsgesellschaft. Leipzig, Becker und Erler, 1943. 469 p.

19. Mador, Irving L. and Ruth S. Quinn. The influence of temperature and state on infrared absorption spectra: Methyl iodide. Journal of Chemical Physics 20: 1837-1842. 1952.

20. Matthias, B.T. and J.P. Remeika. Ferroelectricity in ammonium sulfate. Physical Review 103: 262-263. 1956.

21. Myasnikova, T.P. and A.F. Yatsenko. Changes in infrared spectra of NH_4HSO_4, $RbHSO_4$, and $(NH_4)_2SO_4$ during ferroelectric transitions. Fizika Tverdogo Tela 4: 653-656. 1962.

22. Oden, Laurance L. and J.C. Decius. The infrared spectrum of ammonium thiocyanate from 90 to $300^\circ K$. Spectrochimica Acta 20: 667-674. 1964.

23. Okaya, Y., K. Vedam, and R. Pepinsky. Non-isomorphism of ferroelectric phases of ammonium sulfate and ammonium fluoberyllate. Acta Crystallographica 11: 307. 1958.

24. Pepinsky, R. and K. Vedam. Ferroelectric transition in rubidium bisulfate. Physical Review 117: 1502. 1960.

25. Pepinsky, R. et al. Ammonium hydrogen sulfate: A new ferroelectric with low coercive field. Physical Review 111: 1508-1510. 1958.

26. Pimentel, George C. and Aubrey L. McClellan. The hydrogen bond. San Francisco, Freemen. 1960. 475 p.

27. Pohlman, R. Ultrarotspektren von Ammoniumsalzen in Gebiet ihrer anomalen spezifischen Wärme. Zeitschrift für Physik 79: 394-420. 1932.

28. Reid, C. Semiempirical treatment of the hydrogen bond. Journal of Chemical Physics 30: 182-190. 1959.

29. Rundle, R.E. and Matthew Parasol. OH stretching frequencies in very short and possibly symmetrical hydrogen bonds. Journal of Chemical Physics 20: 1487-1488. 1952

30. Siebert, Hans. Schwingungsspektren einiger Derivate der Schwefelsaüre. Zeitschrift für Anorganische und Allegemeine Chemie 289: 15-28. 1957.

31. Singh, Bachchan. Ferroelectricity and the structural mechanism of the ammonium sulfate transition. Ph.D. Thesis. State College, The Pennsylvania State University, 1962. 234 numb. leaves.

32. Stakhanov, A.I., and Z.A. Gabrichidze. Raman spectra in a ferroelectric ammonium sulfate crystal. Fizika Tverdogo Tela. 5(11): 3105-3109. 1963.

33. Swenson, C.A. et al. Infrared studies of crystal benzene. I. The resolution and assignment of ν 20 and the relative magnitudes of crystal fields in benzene. Journal of Chemical Physics 31: 1324-1328. 1959.

34. Thrierr, Jean Claude. Spectre Raman du sulfate d'ammonium a température ordinaire. Comptes Rendus des Séances de l'Académie des Sciences 253: 2917-2918. 1961.

35. Tramer, André. Spectres de vibration et structure des cristaux de sulfocyanure d'ammonium. Comptes Rendus des Séances de l'Académie des Sciences 249: 2755-2757. 1959.

36. Wagner, E.L. and D.F. Hornig. The vibrational spectra of molecules and complex ions in crystals III. Ammonium chloride and deutero-ammonium chloride. Journal of Chemical Physics 18: 296-304. 1950.

37. ―――――――――The vibrational spectra of molecules and complex ions in crystals IV. Ammonium bromide and deutero-ammonium bromide. Journal of Chemical Physics 18: 305-312. 1950.

38. Walrafen, G.E., D.E. Irish, and T.F. Young. Raman studies of molten potassium bisulfate and vibrational frequencies of $S_2O_7^=$ groups. Journal of Chemical Physics 37: 662-670. 1962.

39. Wilson, E. Bright Jr. A method of obtaining the expanded secular equation for the vibration frequencies of a molecule. Journal of Chemical Physics 7: 1047-1052. 1939.

40. Wilson, E. Bright Jr., J.C. Decius, and Paul C. Cross. Molecular Vibrations. New York. McGraw-Hill. 1955. 370 p.

41. Winston, Harvey and Ralph S. Halford. Motions of molecules in condensed systems: V. Classification of motions and selection rules for spectra according to space symmetry. Journal of Chemical Physics 17: 607-616. 1949.

42. Zvankova, Z.V. and G.S. Zhdanov. X-ray study of ammonium thiocyanate. Zhurnal Fizicheskoi Khimii 23: 1495-1501. 1949.

43. Zwerdling, Solomon and Ralph S. Halford. Motions of molecules in condensed systems: IX. Infrared absorption anisotropy and induced molecular motion in a single crystal of benzene. Journal of Chemical Physics 23: 2221-2228. 1955.

VII.   APPENDIX I

Ammonium Ion Potential Function

Consider the XY_4 model as labeled in figure 16.

Figure 16.   Tetrahedral XY_4 model

In terms of internal coordinates Δr and ΔR, where Δr and ΔR designate small changes in bonded $X - Y$ and nonbonded $Y - Y$ distances respectively, the compliance matrix has the form below. In order to have complete sets of internal coordinates, a total of ten coordinates is needed.

C	Δr_1	Δr_2	Δr_3	Δr_4	ΔR_{12}	ΔR_{13}	ΔR_{14}	ΔR_{23}	ΔR_{24}	ΔR_{34}
Δr_1	C_r	C_r'	C_r'	C_r'	C_{rR}	C_{rR}	C_{rR}'	C_{rR}'	C_{rR}'	C_{rR}'
Δr_2		C_r	C_r'	C_r'	C_{rR}	C_{rR}'	C_{rR}'	C_{rR}	C_{rR}	C_{rR}'
Δr_3			C_r	C_r'	C_{rR}'	C_{rR}	C_{rR}'	C_{rR}'	C_{rR}'	C_{rR}
Δr_4				C_r	C_{rR}'	C_{rR}'	C_{rR}	C_{rR}'	C_{rR}	C_{rR}
ΔR_{12}					C_R	C_R'	C_R'	C_R'	C_R'	C_R''
ΔR_{13}						C_R	C_R'	C_R''	C_R''	C_R'
ΔR_{14}							C_R	C_R''	C_R'	C_R'
ΔR_{23}								C_R	C_R'	C_R'
ΔR_{24}									C_R	C_R'
ΔR_{34}										C_R

The G matrix has identical form: a typical element of G, written g_{ij}, corresponds in position to the c_{ij} element of C. Both C and G are symmetric matrices; hence only those elements on and above the principle diagonal have been entered.

The elements of G are readily calculated (see 40, p. 303-306).

$$g_r = \mu x + \mu y \qquad\qquad g_{R''} = 0$$

$$g_{r'} = -\mu x/3 \qquad\qquad g_{rR} = (2/3)^{\frac{1}{2}}\mu y$$

$$g_R = 2\mu y \qquad\qquad g_{rR'} = 0$$

$$g_{R'} = \mu y/2$$

The XY_4 model has tetrahedral symmetry, point group T_d, and the completely reduced representation of T_d contains the symmetry species $A_1 + E + 2F_2$. Introduction of the following set of symmetry coordinates factors the compliance and G matrices into a linear factor A_1, a linear factor E, and a quadratic factor $2F_2$.

$$S_1 = S^{A1} = \tfrac{1}{2}(\Delta r_1 + \Delta r_2 + \Delta r_3 + \Delta r_4)$$

$$S_2 = S^{A1} = 6^{-\frac{1}{2}}(\Delta R_{12} + \Delta R_{13} + \Delta R_{14} + \Delta R_{23} + \Delta R_{24} + \Delta R_{34})$$

$$S_3 = S^{E} = 12^{-\frac{1}{2}}(2\Delta R_{12} - \Delta R_{13} - \Delta R_{14} - \Delta R_{23} - \Delta R_{24} + 2\Delta R_{34})$$

$$S_4 = S^{F2} = \tfrac{1}{2}(\Delta r_1 + \Delta r_2 - \Delta r_3 - \Delta r_4)$$

$$S_5 = S^{F2} = 2^{-\frac{1}{2}}(\Delta R_{12} - \Delta R_{34})$$

S_2 is a redundant coordinate in the A_1 species and need not be included; however it will be applicable later.

The symmetrized compliance matrix, $\mathbb{C}$, has the following form.

$\mathbb{C}$	S_1	S_3	S_4	S_5
S_1	C_r+3C_r'	0	0	0
S_3		$C_R-2C_R'+C_R''$	0	0
S_4			C_r-C_r'	$2^{\frac{1}{2}}(C_{rR}-C_{rR}')$
S_5				C_R-C_R''

The elements of $\mathbb{G}$ are identical in form to corresponding elements of $\mathbb{C}$. Inversion of $\mathbb{G}$ produces the $\mathbb{K}$ matrix.

$\mathbb{K}$	S_1	S_3	S_4	S_5
S_1	m_y	0	0	0
S_3		m_y	0	0
S_4			$3m_x m_y/M$	$-3^{\frac{1}{2}}m_x m_y/M$
S_5				$[(3/2)m_x+2m_y]\,m_y\,/M$

M is the total mass of the molecule.

Expansion of the secular equation $\left|\mathbb{K}\,\mathbb{C}-\bar{\Phi}\,\mathbb{E}\right|=0$ yields the following equations.

A_1: (I-1) $C_r+3C_r' = \phi_1/m_y$

E : (I-2) $C_R-2C_R'+C_R'' = \phi_2/m_y$

F_2: (I-3) $3m_x(C_r-C_r')-2(6)^{\frac{1}{2}}m_x(C_{rR}-C_{rR}')+[(3/2)m_x+2m_y]$
$$[C_R-C_R''] = M(\phi_3+\phi_4)/m_y$$

(1-4) $(C_r-C_r')(C_R-C_R'')-2(C_{rR}-C_{rR}')^2 = 2M\phi_3\phi_4/3m_x m_y^2$

Equations I-3 and I-4 were obtained by applying the relations $\phi_3+\phi_4 = \sum(KC)_{ii}$ and $\phi_3\phi_4 = \det(KC)$, respectively, to the F_2 species of the secular equation.

Decius (6) has shown that two additional equations can be obtained from the A_1 species by using the redundant coordinate S_2. The relations are:

(I-5) $6^{\frac{1}{2}}(C_{r_R}+C_{r_R}') = 2\phi_1 /m_y$

(I-6) $C_R+4C_R'+C_R'' = 4\phi_1 /m_y$

The degenerate vibrations ω_2^+, ω_3^+, and ω_4^+ exhibited multiple components in the spectra observed at low temperature; hence the frequencies used in the calculations were taken as the averages of the degenerate components. Calculations are facilitated if compliance constants and atomic masses are entered with units of angstroms per millidyne and atomic mass units respectively; then $\phi_i = (1303.1 /\omega_i)^2$. The following values were used in the calculations: $m_H = 1.000$, $m_D = 2.000$, $m_N = 14.000$.

Table two of the text lists the average frequencies used and the compliance constants obtained by solution of the set of equations I-1 through I-6. Due to anharmonicity, a single set of constants would not produce an exact fit to both NH_4^+ and ND_4^+ frequencies. Therefore, two sets of constants were calculated, one set to fit NH_4^+ and the other to fit ND_4^+.

The vibrational frequency for $\omega_1{}^+$, as listed in table two, was calculated as follows using the observed NH stretching frequency of $NHD_3{}^+$, 3090 cm^{-1} in figure four. Substitution into the classical expression $\nu = c\omega = 1/2\pi(fr/m_{eff})^{\frac{1}{2}}$, where $m_{eff} = m_H m_N / m_H + m_N$, yields a value of 5.25 mdynes $/\overset{o}{A}$ for f_r. It is known (40, p. 74-76) that a good approximation to the high frequency vibrations can be obtained by deleting all rows and columns from F and G which concern the low frequency modes. In the case of XY_4 this amounts to reducing F to

$$\begin{pmatrix} f_r+3f_r{}' & 0 \\ 0 & f_r-f_r{}' \end{pmatrix}$$

which corresponds to an A_1 and an F_2 stretching vibration. G has identical form, and on substitution of the appropriate elements becomes:

$$\begin{pmatrix} \mu_y & 0 \\ 0 & (4/3)\mu_x+\mu_y \end{pmatrix}.$$

Expansion of the secular equation $|F G - \lambda E| = 0$ yields:

(I-7) $(f_r+3f_r{}')\mu_y = \lambda_1$

(I-8) $(f_r-f_r{}')(4\mu_x/3 + \mu_y) = \lambda_3$

f_r was calculated above and $\omega_3{}^+$ was observed (3070 cm^{-1}); hence the above equations can be solved for the missing A_1 vibration, $\omega_1{}^+$.

VIII. APPENDIX II

Vibrational Frequencies of Partially Deuterated Ammonium Ions

A: XYZ_3 type with C_{3v} symmetry
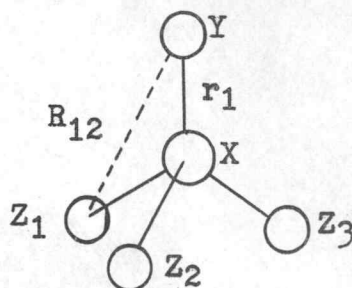
Consider the model of figure 17.

Figure 17. C_{3v} model

Internal coordinates have been chosen to coincide with the tetrahedral model of appendix I. The compliance matrix in internal coordinates has the following form where compliance constants have been designated by appending small zero superscripts to the corresponding constants for the tetrahedral model.

c	Δr_1	Δr_2	Δr_3	Δr_4	ΔR_{12}	ΔR_{13}	ΔR_{14}	ΔR_{23}	ΔR_{24}	ΔR_{34}
Δr_1	c_r	$c_r^{o'}$	$c_r^{o'}$	$c_r^{o'}$	c_{rR}^{oo}	c_{rR}^{oo}	c_{rR}^{oo}	$c_{rR}^{o'}$	$c_{rR}^{o'}$	$c_{rR}^{o'}$
Δr_2		c_r	$c_r^{'}$	c_r^{o}	c_{rR}^{o}	$c_{rR}^{o'}$	$c_{rR}^{o'}$	c_{rR}	c_{rR}	$c_{rR}^{'}$
Δr_3			c_r	$c_r^{'}$	$c_{rR}^{o'}$	c_{rR}^{o}	$c_{rR}^{o'}$	c_{rR}	$c_{rR}^{'}$	c_{rR}
Δr_4				c_r	$c_{rR}^{o'}$	$c_{rR}^{o'}$	c_{rR}^{o}	$c_{rR}^{'}$	c_{rR}	c_{rR}
ΔR_{12}					c_R^{oo}	$c_R^{oo'}$	$c_R^{oo'}$	$c_R^{o'}$	$c_R^{o'}$	$c_R^{o''}$
ΔR_{13}						c_R^{oo}	$c_R^{oo'}$	$c_R^{o'}$	$c_R^{o''}$	$c_R^{o'}$
ΔR_{14}							c_R^{oo}	$c_R^{o''}$	$c_R^{o'}$	$c_R^{o'}$
ΔR_{23}								c_R	$c_R^{'}$	$c_R^{'}$
ΔR_{24}									c_R	$c_R^{'}$
ΔR_{34}										c_R

From the correlation theorem of figure seven it is known that $\Gamma_{C_{3v}} = 3A_1 + 3E$. Convenient symmetry coordinates are formed as follows.

$$S_1 = S_1{}^{A_1} = \Delta r_1$$
$$S_2 = S_2{}^{A_1} = \bar{3}^{\frac{1}{2}} (\Delta r_2 + \Delta r_3 + \Delta r_4)$$
$$S_3 = S_3{}^{A_1} = \bar{3}^{\frac{1}{2}} (\Delta R_{12} + \Delta R_{13} + \Delta R_{14})$$
$$S_4 = S_1{}^{E} = \bar{6}^{\frac{1}{2}} (2\Delta r_2 - \Delta r_3 - \Delta r_4)$$
$$S_5 = S_2{}^{E} = \bar{6}^{\frac{1}{2}} (2\Delta R_{12} - \Delta R_{13} - \Delta R_{14})$$
$$S_6 = S_3{}^{E} = \bar{6}^{\frac{1}{2}} (2\Delta R_{34} - \Delta R_{23} - \Delta R_{24})$$

The symmetrized compliance matrix has the following form.

$\mathbb{C}$	S_1	S_2	S_3	S_4	S_5	S_6
S_1	C_r^{oo}	$3^{\frac{1}{2}}C_r^{o'}$	$3^{\frac{1}{2}}C_{rR}^{oo}$	0	0	0
S_2		$C_r + 2C_r'$	$C_{rR}^{o} + 2C_{rR}^{o'}$	0	0	0
S_3			$C_R^{oo} + 2C_R^{oo'}$	0	0	0
S_4				$C_r - C_r'$	$C_{rR}^{o} - C_{rR}^{o'}$	$C_{rR}' - C_{rR}$
S_5					$C_R^{oo} - C_R^{oo'}$	$C_R^{o''} - C_R^{o'}$
S_6						$C_R - C_R'$

The symmetrized $\mathbb{G}$ matrix has identical form.

$\mathbb{G}$	S_1	S_2	S_3	S_4	S_5	S_6
S_1	$\mu_x + \mu_y$	$\mu_x/3^{\frac{1}{2}}$	$2^{\frac{1}{2}}\mu_y$	0	0	0
S_2		$\mu_z + \mu_x/3$	$(2/3)^{\frac{1}{2}}\mu_z$	0	0	0
S_3			$2\mu_y + \mu_z$	0	0	0
S_4				$4\mu_x/3 + \mu_z$	$(2/3)^{\frac{1}{2}}\mu_z$	$-(2/3)^{\frac{1}{2}}\mu_z$
S_5					$\mu_z + \mu_y/2$	$\mu_z/2$
S_6						$3\mu_z/2$

In the calculation of frequencies of vibration of partially deuterated species, an attempt was made to correct for anharmonicity by adjusting compliance constants by equation II - 1.

II - 1 $C_{H_p D_{4-p}} = (pC_{H_4^+} + (4-p)C_{D_4})/4$

In numerical form, $\mathbb{C}$ and $\mathbb{G}$ are as follows:

NH_3D^+:

$\mathbb{C}$	S_1	S_2	S_3	S_4	S_5	S_6
S_1	0.2056	-0.0190	0.1974			
S_2		0.1836	0.1674			
S_3			0.6749			
S_4				0.2166	0.0873	-0.0873
S_5					0.6302	-0.0302
S_6						0.6302

$\mathbb{G}$						
S_1	0.5714	-0.0412	0.7071			
S_2		1.0238	0.8164			
S_3			2.0000			
S_4				1.0952	0.8164	-0.8164
S_5					1.2500	-0.5000
S_6						1.5000

NHD_3^+

C	S_1	S_2	S_3	S_4	S_5	S_6
S_1	0.2010	−0.0164	0.1943			
S_2		0.1820	0.1692			
S_3			0.6748			
S_4				0.2105	0.0837	−0.0837
S_5					0.6265	−0.0339
S_6						0.6265

G	S_1	S_2	S_3	S_4	S_5	S_6
S_1	1.0714	−0.0412	1.4142			
S_2		0.5238	0.4082			
S_3			2.5000			
S_4				0.5952	0.4082	−0.4082
S_5					1.0000	−0.2500
S_6						0.7500

Calculation of the frequencies was accomplished by the 7090 computor of U.C.L.A., using the HDIAG subroutine. Frequencies are listed in table three of the text.

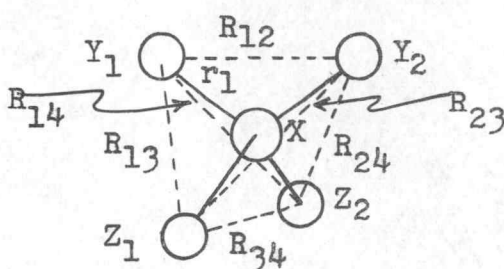B: XY_2Z_2 type with C_{2v} symmetry

Figure 18. C_{2v} model

The internal coordinates fall into five symmetrically complete sets: $(\Delta r_1, \Delta r_2), (\Delta r_3, \Delta r_4), (\Delta R_{12}), (\Delta R_{13}, \Delta R_{14}, \Delta R_{23}, \Delta R_{24}), (\Delta R_{34})$ from which symmetry coordinates are formed. From the correlation theorem of figure seven, it is known that $\Gamma_{C_{2v}} = 4A_1 + A_2 + 2B_1 + 2B_2$.

Symmetry coordinates are formed as follows:

$S_1 = S^{A1} = 2^{-\frac{1}{2}}(\Delta r_1 + \Delta r_2)$

$S_2 = S^{A1} = 2^{-\frac{1}{2}}(\Delta r_3 + \Delta r_4)$

$S_3 = S^{A1} = \Delta R_{12}$

$S_4 = S^{A1} = \Delta R_{34}$

$S_5 = S^{A2} = \frac{1}{2}(\Delta R_{13} - \Delta R_{14} - \Delta R_{23} + \Delta R_{24})$

$S_6 = S^{B1} = 2^{-\frac{1}{2}}(\Delta r_1 - \Delta r_2)$

$S_7 = S^{B1} = \frac{1}{2}(\Delta R_{13} + \Delta R_{14} - \Delta R_{23} - \Delta R_{24})$

$S_8 = S^{B2} = 2^{-\frac{1}{2}}(\Delta r_3 - \Delta r_4)$

$S_9 = S^{B2} = \frac{1}{2}(\Delta R_{13} - \Delta R_{14} + \Delta R_{23} - \Delta R_{24})$

The compliance and G matrices in internal coordinates contain an excessive number of symbols; therefore suffice it to include only the symmetrized matrices. Also, since only one C_{2v} ion exists, NH_2D_2+, the XY_2Z_2 symbolism will be dispensed with.

c

$$\begin{pmatrix}
C_r+C_r' & 2C_r' & 2^{\frac{1}{2}}C_{rR} & 2^{\frac{1}{2}}C_{rR}' & 0 & 0 & 0 & 0 & 0 \\
 & C_r+C_r' & 2^{\frac{1}{2}}C_{rR}' & 2^{\frac{1}{2}}C_{rR} & 0 & 0 & 0 & 0 & 0 \\
 & & C_R & C_R'' & 0 & 0 & 0 & 0 & 0 \\
 & & & C_R & 0 & 0 & 0 & 0 & 0 \\
 & & & & C_R+C_R'' & 0 & 0 & 0 & 0 \\
 & & & & & C_r-C_r' & 2^{\frac{1}{2}}(C_{rR}-C_{rR}') & 0 & 0 \\
 & & & & & & C_R-C_R'' & 0 & 0 \\
 & & & & & & & C_r-C_r' & 2^{\frac{1}{2}}(C_{rR}-C_{rR}') \\
 & & & & & & & & C_R-C_R''
\end{pmatrix}$$

d

$$\begin{pmatrix}
2\mu_N/3+\mu_H & -2\mu_N/3 & 2\mu_H/3^{\frac{1}{2}} & 0 & 0 & 0 & 0 & 0 & 0 \\
 & 2\mu_N/3+\mu_D & 0 & 2\mu_D/3^{\frac{1}{2}} & 0 & 0 & 0 & 0 & 0 \\
 & & 2\mu_H & 0 & 0 & 0 & 0 & 0 & 0 \\
 & & & 2\mu_D & 0 & 0 & 0 & 0 & 0 \\
 & & & & (\mu_H+\mu_D)/2 & 0 & 0 & 0 & 0 \\
 & & & & & 4\mu_N/3+\mu_H & 2\mu_H/3^{\frac{1}{2}} & 0 & 0 \\
 & & & & & & (3\mu_H+\mu_D)/2 & 0 & 0 \\
 & & & & & & & 4\mu_N/3+\mu_D & 2\mu_D/3^{\frac{1}{2}} \\
 & & & & & & & & (3\mu_D+\mu_H)/2
\end{pmatrix}$$

The elements of $\mathfrak{G}$ have been adjusted by equation II - 1, and numerically $\mathfrak{C}$ and $\mathfrak{G}$ are as follows:

$\mathfrak{C}$

0.1930	-0.0206	0.1599	0.0390	0	0	0	0	0
-0.0206	0.1930	0.0390	0.1599	0	0	0	0	0
0.1599	0.0390	0.6439	-0.0166	0	0	0	0	0
0.0390	0.1599	-0.0166	0.6439	0	0	0	0	0
				0.6273	0	0	0	0
					0.2136	0.1209	0	0
					0.1209	0.6605	0.2136	0.1209
							0.1209	0.6605

$\mathfrak{G}$

1.0476	-0.0476	1.1546	0	0	0	0	0	0
-0.0476	0.5476	0	0.5773	0	0	0	0	0
1.1546	0	2.0000	0	0	0	0	0	0
0	0.5773	0	1.0000	0	0	0	0	0
				0.7500	0	0	0	0
					1.0952	1.1546	0	0
					1.1546	1.7500	0	0
							0.5952	0.5773
							0.5773	1.2500

As in the case of XYZ_3 type ions, the frequencies were calculated by the U.C.L.A. computor. Frequencies are listed in table three of the text.